Characterization of Mrc1 during Replication Initiation in *Saccharomyces cerevisiae*

by

Bradley D'souza

A thesis

presented to the University of Waterloo

in fulfillment of the

thesis requirement for the degree of

Master of Science

in

Biology

Waterloo, Ontario, Canada, 2022

Author’s Declaration

I hereby declare that I am the sole author of this thesis. This is a true copy of the thesis, including any required final revisions, as accepted by my examiners.

I understand that my thesis may be made electronically available to the public.

Abstract

DNA replication is a highly specific process that is completed under the control of several factors, to ensure faithful duplication of the genome. Mrc1 (Claspin in mammalian cells) is a protein that is a part of a fork protection complex (FPC) to stabilize the association between the replisome and DNA as replication takes place. Mrc1 also mediates the intra-S phase cell cycle checkpoint response to resolve replicative stress, facilitating Mec1 sensor kinase phosphorylation of Rad53 effector kinase. Recent studies have revealed a potential role of Mrc1 in the regulation of origin firing timing through interactions with Dbf4-dependant kinase (DDK). DDK is required for replication initiation, phosphorylating Mcm2-7 helicase at origins of replication. DDK is composed of Cell division cycle 7 (Cdc7), the kinase component, and Dumbbell forming unit 4 (Dbf4), the regulatory subunit which activates Cdc7 once bound. Mrc1/Claspin binding to Cdc7 has been characterized in several model organisms but work in this thesis aims to specify the relatively uncharacterized interaction in *Saccharomyces cerevisiae*, also known as budding yeast.

Initial yeast-two hybrid (Y2H) results confirm an interaction of budding yeast Mrc1 with Dbf4, rather than Cdc7. This implicates the possibility of a novel mechanism in regulating DNA replication in a checkpoint-independent fashion. Successive Y2H trials with several truncations of Mrc1 have revealed a distinct N1.1 region (amino acid residues 1 – 186) that is necessary and sufficient for binding to Dbf4. An Mrc1 ΔN1.1 strain was generated and subjected to growth curve trials to assess the phenotypic effect of this mutant under optimal growth conditions. Growth curve analysis revealed a consistent Mrc1 ΔN1.1

growth defect in comparison to wildtype cells in the absence of genotoxic stressors, supporting a checkpoint-independent role of Mrc1. Checkpoint response was subsequently assessed to ensure that the growth defect is not due to potential disruptions in the Rad53 kinase cascade pathway. A spot plate assay amongst various genotoxic stressors showed consistent Mrc1 ΔN1.1 growth to wildtype levels and significantly more growth in comparison to a ΔMrc1 strain. These results indicate intact checkpoint functionality, despite a growth curve defect that is speculated to be due to reduced DNA replication initiation. Overall, these results indicate that Mrc1 ΔN1.1 is a separation of function mutant between its role in DNA replication initiation and checkpoint response.

Characterization of Mrc1 ΔN1.1 S-phase progression was conducted to specify the source of checkpoint-independent growth defect. Fluorescence-activated cell sorting (FACS) analysis results showed no significant differences in S-phase progression. However, plasmid stability assay results displayed a higher rate of average plasmid loss per generation within Mrc1 ΔN1.1 cells in comparison to wildtype. This confirms a minor deficiency in DNA replication which was not distinguishable in prior FACS analysis. In comparison to previous studies, findings outlined in this thesis confirm and further characterize distinct Mrc1-DDK binding in budding yeast, which is required for optimal growth rates and DNA replication stability. Further insight of this interaction will help distinguish between Mrc1s role in checkpoint response and normal DNA replication, which has implications in the development of clinical therapeutics for tumor cell lines with DDK overexpression.

Acknowledgements

First, I would like to thank my supervisor, Dr. Bernard Duncker. Throughout the years in your lab, you have always pushed me to strive for my best and I have learned so much from it. I am grateful for the mentorship and guidance you have provided me in not only research, but life skills that will stay with me throughout my career. Thank you to Dr. Christine Dupont and Dr. Dale Martin for being my committee members. Your valuable input has also helped steer me in the right direction throughout my program.

Thank you to my mentor early in my graduate career, Larasati. From answering my questions (there were a lot!) to helping me navigate myself in the lab, you always took time out of your day to help me. To other lab members I worked with throughout the years, thank you for your assistance in so many ways. It was a pleasure to work with both Mike Meleka and Justin Law on the Mrc1 project. Thank you for the contributions and insight throughout the entire process.

Thank you to my close friends Mufaddal Darikee, Matthew Kerner and Mark Fung. The three of you always kept me laughing at every step of the way and were there for me whenever I needed it.

Finally, I would like to give a big thank you to my family. To my parents Austin and Janet, you have always supported me in my endeavors throughout my life and I am forever grateful for your support. To my brother Calvin, you have been a fantastic role model and I promise to pay you back for all the French vanillas when I visited home!

Table of Contents

List of Tables

List of Figures

List of Abbreviations and Acronyms

APC: Anaphase promoting complex/cyclosome

AQ: Alanine-Glutamine

ARS: Autonomously replicating sequence

CDC: Cell division cycle

CDK: Cyclin-dependant kinase

ChIP: Chromatin immunoprecipitation

CMG: Cdc45, Mcm2-7, GINS

DDK: Dbf4-dependant kinase

dNTP: Deoxynucleotide phosphate

FACS: Fluorescence-Activated Cell Sorting

FPC: Fork protection complex

FL: Full length

HBS: Hsk1 bypass segment

HU: Hydroxyurea

IDR: Intrinsically disordered region

IN: Input sample

IP: Immunoprecipitate sample

KB: Kilobase

kDa: Kilodalton

LB: Lysogeny broth

MCM: Minichromosome maintenance

MMS: Methyl methanesulfonate

MPC: Magnetic particle concentrator

NSD: N-terminal Serine/Threonine rich domain

NTHBS: N-terminal target of HBS

OGRE: Origin G-rich Repeated Element

ONP: Ortho-nitrophenyl

ONPG: Ortho-Nitophenyl-ß-galatoside

ORC: Origin recognition complex

PCR: Polymerase Chain Reaction

Pre-RC: Pre-replicative complex

SC: Synthetic complete

SQ/TQ: Serine-Glutamine/Threonine-Glutamine

ssDNA: Single-stranded DNA

WCE: Whole cell extract

Y2H: Yeast two-hybrid

YPD: Yeast extract, peptone, dextrose

Chapter 1: Introduction

1.1 Background

1.1.1 *Saccharomyces cerevisiae* as a Model Organism

Yeast are historically significant unicellular eukaryotes, instrumental in various industries throughout human civilization such as winemaking and baking. Yeast are non-photosynthetic, utilizing varying organic compounds as carbon and energy sources based upon availability (reviewed in Tomova *et al.*, 2019). As a result, they are found in diverse habitats ranging from aquatic ecosystems to animal intestinal tracts. Yeast are members of the fungi kingdom and over 2000 species are currently identified (Radecka *et al.*, 2015). Importantly, they have also served as a model organism in the study of fundamental cellular processes. The study of yeast at a genetic level began in the mid-1930s with the introduction of fundamental techniques to study single cells by Øjvind Winge, often referred to as the father of yeast genetics (reviewed in Szybalski, 2001). For example, Winge began micromanipulation of spores by separating them into separate droplets using fine glass needles. Furthermore, development of consistent methods for tetrad analysis showed that yeast alternate between haploid and diploid phases. Combined with the discovery of yeast mating, fermentation characteristics could be manipulated for industrial uses (reviewed in Maicas, 2020). Since then, various species of yeast have been used to further our understanding in diverse areas of research such as DNA replication.

Saccharomyces cerevisiae, also termed budding yeast, is an example of a popular model organisms that has furthered our understanding of cell cycle and cancer research. The term “budding yeast” is derived from its mode of asexual reproduction, where daughter cells

are formed through a bud that grows and pinches off from the original mother cells (reviewed in Wang *et al.*, 2017). Several features of budding yeast are well suited for laboratory use. Firstly, budding yeast typically have a doubling time of 90 minutes when grown at 30°C on YPD (1% yeast extract, 2% peptone, and 2% dextrose), a complete media which supports optimal growth. Budding yeast is also considered a safe and generally non-pathogenic microorganism. As a result, it can be grown quickly and safely without any specialized precautions needed to complete experiments in a timely manner. Furthermore, *S. cerevisiae* is a versatile organism for a wide range of studies due to the ease of genetic manipulation with the complete sequencing of its genome in 1996 (Gofeau *et al.*, 1996). The S288C yeast strain was used in this study, which is a widely used strain due to several benefits such as a minimal set of nutritional requirements (reviewed in Engel and Cherry 2013). Coupled with the high rates of homologous recombination, genomic integrations in this strain can be made readily to modify gene expression or epitope tagging. For example, epitope tagging can be completed using primers which amplify a cassette containing a tag and a selection marker. These primers also contain homologous sequences to the regions flanking the C-terminus of the gene of interest, recombining at the gene end, and creating a tagged protein. Additionally, circular plasmids can be transformed to express genes of interest on selective media (discussed in further detail in *1.1.2 Budding Yeast Genetics*).

Budding yeast are also suitable candidates for the study of cell cycle progression due to the ease in inducing cell cycle arrest. Haploid budding yeast cells are present in either MATα or MATa mating types, determined by transcriptional activity of a mating type

(MAT) locus (reviewed in Haber, 2012). Cells of the one mating type secrete a distinct pheromone, which binds to receptors of cells with the opposing mating type. For example, MATa cells release a-factor pheromone, which binds to MATα cell receptors. This initiates a mating response, where cells undergo a pathway to form outward projections, colloquially referred to as called a "schmoo" phenotype, that eventually combine to form a diploid cell (reviewed in Kruckeberg and Dickinson, 2004). Importantly, this process arrests cells in G1 phase and researchers manipulate this feature to study relative cell cycle progression amongst various yeast strains. Specifically, several MATa cell cultures can be resuspended in media containing α-factor, which would induce cell cycle arrest in G1 phase. α-factor would then need to be degraded to release cells from arrest and allow for comparative analysis of cell cycle progression, often through the addition of a protease mixture from Streptomyces Griseus, called Pronase E. Budding yeast has proven to be a pivotal model organism in the study of cell cycle and cancer research, that can then be applied to higher eukaryotes. For example, Leland Hartwell and colleagues used *S. cerevisiae* to understand cell division cycle (CDC) genes, which are responsible for the progression of eukaryotic cell cycle (Pulverer, 2001). Hartwell, alongside Paul Nurse (*Schizosaccharomyces pombe* studies) and Timothy Hunt (*Arbacia punctulate* studies), shared a Nobel Prize in 2001 for their discoveries and characterization of DNA replication regulation in various model organisms. Therefore, it is evident that budding yeast has played a pivotal role in the advancement of cell cycle research in the past and will remain a relevant model for years to come.

1.1.2 Budding Yeast Genetics

The genome of *S. cerevisiae* is 12,068 kilobases in size, organized into 16 chromosomes (Goffeau, *et al.*, 1996). The complete sequencing of the budding yeast genome is a powerful tool in understanding organization and function of genes. Currently, there are 6611 identified open reading frames, of which 5228 encode proteins, 682 are unlikely to encode a functional protein, and 701 remain uncharacterized by experimental data (Saccharomyces Genome Database, 2021). The budding yeast genome is compact, with an approximately 50-fold higher gene density in comparison to the human genome and a low abundance of genes containing introns (4%), a relatively small proportion in comparison to other eukaryotes (Duina *et al*., 2014 and Parenteau et al., 2019).

The ability of budding yeast to live in both diploid and haploid forms is an important feature regarding experimental design. Most notably, diploid cells contain two sets of chromosomes and mutations in a single copy can be masked by wild-type alleles. Haploid cells are primarily preferred due to single mutations creating phenotypic changes that can be readily identified. For example, disruption of an essential gene that results in a loss of its function is lethal in haploid cells. As a result, mutants dependent upon environment conditions were developed as a viable strategy to control gene function, without complete deletion of a gene of interest. A common mutant used for these purposes are thermo-sensitive strains, which causes loss of gene function at non-permissive temperatures. Another advantage of haploid cells is the ability to undergo mating, as mentioned previously. This

feature allows for synchronous arrest and release of cells from various stages of the division process, for cell cycle progression analysis.

Furthermore, common lab strains of *S. cerevisiae* often have mutations in essential genes to create a functional auxotroph. This is done to allow for selection of yeast cells that are transformed with DNA which contains a selectable marker such as URA3 (Saccharomyces Genome Database, 2021). This gene encodes orotidine 5-phosphate decarboxylase (ODCase), an enzyme which is necessary for the synthesis of the essential nucleobase uracil (Lacroute, 1968). Background strains often have a functional mutation of this gene, resulting in a lack of growth in the absence of an exogenous uracil source. These cells can be transformed with a circular plasmid containing a functional URA3 gene. Finally, researchers select for successful transformants which can grow on plates lacking uracil. This is a fundamental technique that is frequently used to select for transformants, which can also include any other genes of interest in the plasmid construct.

1.1.3 Budding Yeast Cell Cycle

Under optimal growth conditions, *S. cerevisiae* cell cycle follows a mitotic division pathway to form identical daughter cells. This mitotic pathway is made up of four primary stages: Gap 1 (G1), Synthesis (S), Gap 2 (G2), and Mitosis (M) (figure 1.1) (Herskowitz, 1988). Budding yeast can also exist as a haploid or diploid, primarily dependent on environmental and growth conditions present. When budding yeast are starved from

necessary nutrients, they will undergo meiosis and sexually reproduce to produce haploid spores (reviewed in Neiman, 2011).

Within the mitotic cell cycle, the primary goals of the G1 phase is to grow in size and produce necessary proteins in preparation for S phase. During late G1 phase, a START checkpoint takes place where cells monitor environmental and internal conditions before further cell cycle progression, such as nutrient availability and cell size, respectively (reviewed in Neiman, 2011). Cyclin proteins also play several roles at this stage to aid in initiation of the mitotic cell cycle, such as repression of mating pathways (Oehlen and Cross, 1994). The START checkpoint is an important process as cells will irreversibly commit to the entire mitotic cycle, regardless of conditions in following stages. If cells are not in a favorable position to complete the cell cycle, they will enter a G0 stationary phase where cells remain dormant until conditions are favorable (Herskowitz, 1988). As mentioned prior, cells can also sexually mate before the START checkpoint to form diploid cells that can undergo either mitotic or meiotic cell cycles.

Pre-replicative complex (pre-RC) formation takes place in G1 phase, which is composed of various proteins that bind to DNA sites where replication initiation begins (reviewed in Bell and Dutta, 2001). This initiation site is called an origin of replication and the process of Pre-RC association is termed origin licensing, which is followed by activation and transformation into the final helicase structure. Phosphorylation by two independent serine-threonine kinases, the cyclin-dependent kinase (CDK) and the Dbf4-dependant kinase

(DDK) facilitate this activation in a process termed “origin firing” (reviewed in Kawasaki *et al.,* 2006). Specific formation details will be discussed in *1.2 Initiation of DNA replication*.

Complete duplication of the genome takes place in S phase, required for the genomic complement in both daughter and mother cells. At this stage pre-RCs are sequentially activated and a catalytic core containing Minichromosome maintenance subunits (Mcm2-7), Cdc45 and GINS complex, or a CMG complex, acts as the minimal active helicase components responsible for separating the parental DNA double helix through two bidirectionally travelling replication forks (reviewed in Riera *et al.*, 2017). Yeast replication protein A is then recruited to each single stranded DNA to prevent reannealing before replication machinery can duplicate these regions. Topoisomerase II is also required downstream of each fork to nick DNA and relieve tension that is generated by the associated fork (reviewed in Kegel *et al.*, 2011). This is an important feature to reduce the likelihood of supercoiled secondary structures that may cause replicative stress.

Following DNA duplication, G2 phase takes place, where cells grow once again and produce proteins required for M phase. Specifically, cells produce proteins involved in mitotic spindle formation, and migration of the nucleus to the bud periphery where nuclear division will take place (reviewed in Segal and Bloom, 2001). The DNA damage checkpoint is also active at the G2/M phase transition to survey for any DNA damage prior to division cellular division. If DNA damage is detected by this checkpoint, cells are prevented from beginning mitosis and employ repair mechanisms, such as a homologous recombination pathway to repair double stranded breaks.

This is followed by M phase, where cell division takes place to form a mother cell and a smaller daughter cell. Mitosis consists of six stages: prophase, prometaphase, metaphase, anaphase, telophase, and cytokinesis. During prophase, chromosomes attach to microtubules at central regions termed kinetochores, which are organized by spindle pole bodies that serve the same functional role as centrosomes in animal cells (Yoder *et al.*, 2003). At this point, the two spindle pole bodies separate to maintain one in the bud and the second in the original mother cell. Chromosomes are then organized in metaphase along at the site of eventual mother and daughter cell division, followed by the activity of the Anaphase Promoting Complex/Cyclosome (APC/C) to initiate anaphase (reviewed in Rudner and Murray, 2000). This complex is an essential ubiquitin ligase that marks the degradation of several cell cycle proteins through an associated Cdc20 protein. Tethering of sister chromatids is established by a cohesin protein complex. The cohesin complex is cleaved by hydrolysis activity of a separase enzyme, which is activated when its inhibitory securin chaperone protein is degraded. Cdc20 facilitates this event, through ubiquitination of securin which targets it for APC/C-mediated degradation. This process allows sister chromatid separation to occur and is a hallmark of anaphase. Additionally, APC/C degrades Dbf4 to prevent additional replication initiation events at this stage of mitosis (Reviewed in Ferreira *et al.*, 2000). During telophase each sister chromatid migrates to opposing spindle poles, the nucleus undergoes conformational changes in preparation for cytokinesis, and continued enlargement of the daughter bud occurs (reviewed in Bell and Dutta, 2001). Finally, cytokinesis is the physical separation of the growing bud from the mother cell that is driven by APC/C activity. At this stage the daughter cell is smaller than the mother cell and will

continue to grow, whereas the mother cell will have a bud scar that remains on its surface (reviewed in Bell and Dutta, 2001).

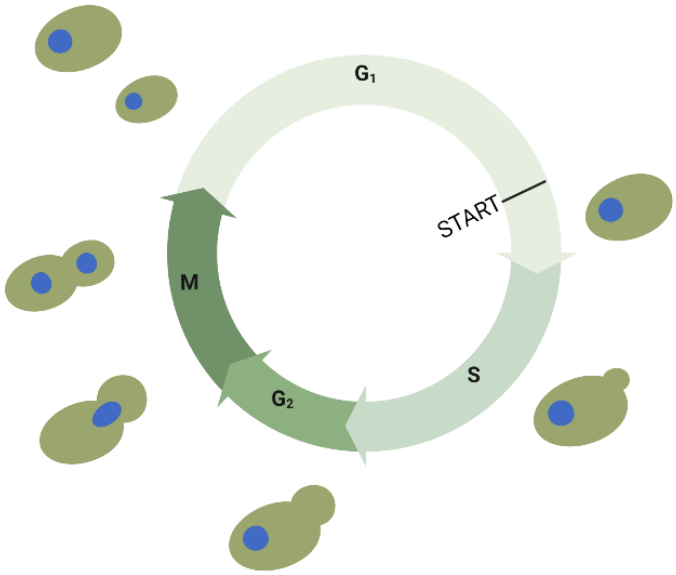

Figure 1.1 *Saccharomyces cerevisiae* mitotic cell cycle. The mitotic cell cycle of budding yeast consists of the following stages: G1, S, G2, and Mitosis (M) (as well as cytokinesis). During late G1 phase a START checkpoint takes place, where yeast assess environmental and internal signals to determine if DNA replication is favorable (reviewed in Neiman, 2011).

1.2 DNA replication Initiation

1.2.1 Origin Licensing

The DNA replication process begins bidirectionally at loci called origins of replication, which are present throughout the genome. Origins were first identified through a plasmid-based assay where segments of the yeast genome were incorporated into bacterial

plasmids (Brewer and Fangman, 1987). If any plasmids replicated when transformed in yeast cells, it was thought to possess an origin site because the original vector construct was not capable of plasmid replication. These sites within the yeast genome were designated as an autonomously replicating sequence (ARS).

As mentioned before, the first step of replication initiation is known as origin licensing. During this step various proteins that form pre-RC are recruited at origins during G1 phase. First, the binding of a six-subunit origin recognition complex (ORC) takes place, which acts as the foundation for the association of subsequent proteins (reviewed in Riera *et al.,* 2017). Next, assembly and binding of cell division cycle 6 (Cdc6) and Chromatin licensing DNA replication factor 1 (Cdt1) to the ORC occurs, which facilitates the binding of two Mcm2-7 hexamers to DNA (Aparicio *et al*., 1997). Cdt1 recruits Mcm2-7 to the origin to be licensed and it is activated by ATP hydrolysis activity of Cdc6, for eventual formation of CMG helicase structure (reviewed by Riera *et al.,* 2017). Once Mcm2-7 hexamers are associated with DNA, origins are considered licensed.

1.2.2 Origin Firing

The next step in DNA replication initiation is called origin firing, which is the transformation of the pre-RC into the active helicase (figure 1.2). Firstly, Cdc45 and GINS proteins are required to begin this transformation and remain associated during elongation. Cdc45 is essential for the binding of replication fork proteins and the four subunit GINS protein complex is required for the interaction between Mcm2-7 subunits and Cdc45 for

eventual formation of the CMG helicase core (reviewed in Riera *et al.*, 2017). The activation of the pre-RC requires phosphorylation by CDK and DDK. DDK is made up of Cell division cycle 7 (Cdc7), the kinase component, and Dumbbell forming unit 4 (Dbf4), the regulatory subunit which activates Cdc7 once bound. Cdc7 phosphorylates Mcm2-7, enabling Sld3-Sld7 and Cdc45 recruitment to the pre-RC (Heller *et al.*, 2011). CDK phosphorylates the proteins Sld2 and Sld3, which form a complex with the scaffold protein Dpb11 at its N- and C-terminus, respectively. This triggers the recruitment and formation of Dpb11, Pol ε, Sld2, and GINS to form a pre-Loading Complex (pre-LC) (reviewed in Muramatsu *et al*., 2010). GINS then associates with origins to form the CMG. Sld7, Sld2, Sld3, and Dpb11 are released from the final CMG and this complex is now the minimum substrate required for helicase activation. Finally, Mcm10 is required to stimulate helicase activity by enhancing CMG binding to DNA (reviewed in Yuan *et al*., 2020). This complex then moves along the DNA in association with DNA polymerase ε, coupling DNA unwinding with DNA synthesis.

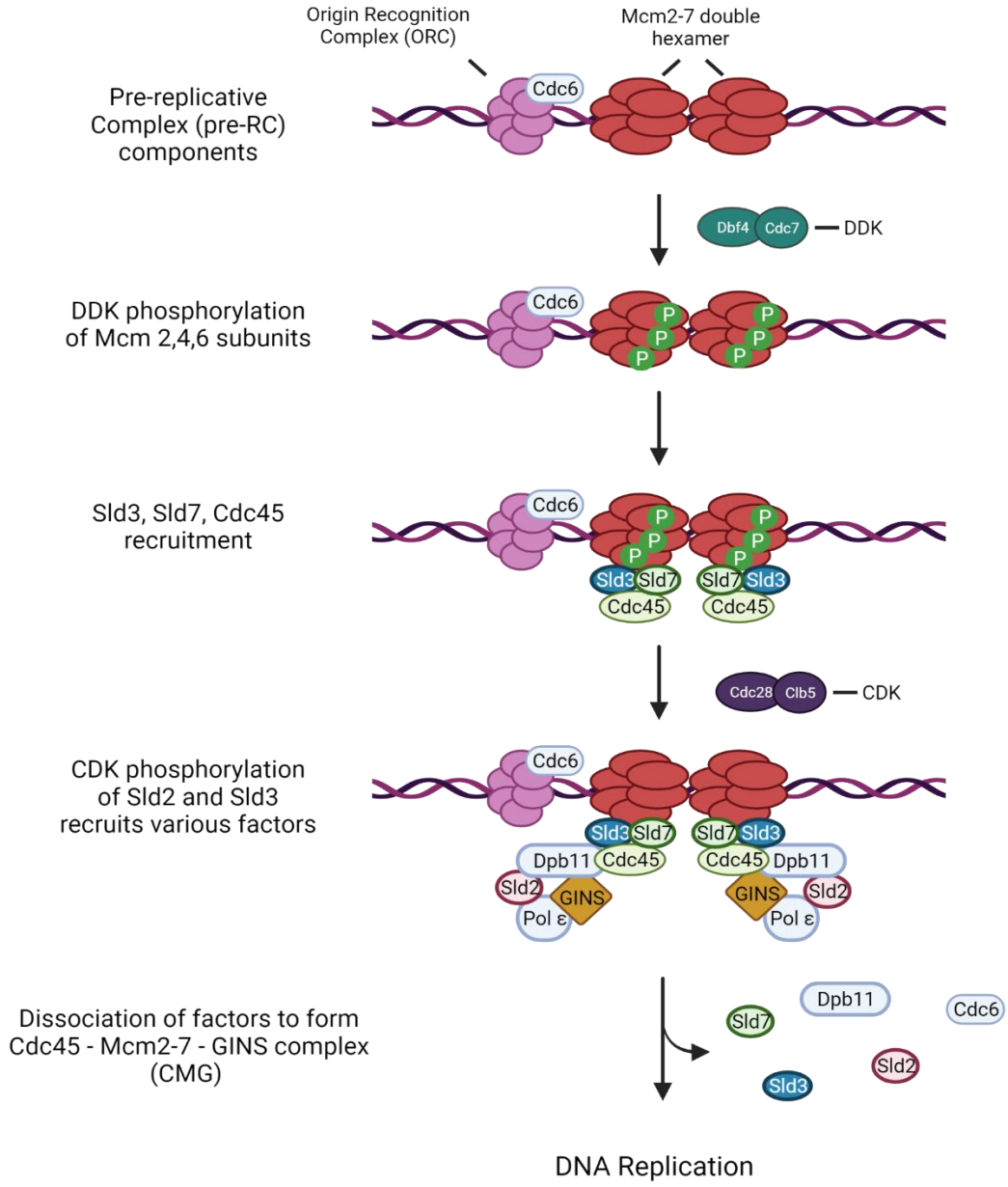

Figure 1.2 Model of Origin Firing in *Saccharomyces cerevisiae.* Following origin licensing and the loading of the pre-RC, origins are fired by DDK and CDK dependent activity. DDK first phosphorylates Mcm2-7 subunits to recruit Sld3, Sld7, and Cdc45 to each hexamer. CDK then phosphorylates Sld2 and Sld3, which form a complex with Dpb11. Subsequently, this leads to GINS and Pol ε recruitment. This process leads to the formation of replication forks that travel bidirectionally from a single origin site (Larasati & Duncker, 2016).

Following kinase activation and CMG formation, an active replication fork is established to carry out DNA replication in a bidirectional fashion. The final structure of the replication fork includes several additional proteins that confer stability and additional features. A fork protection complex (FPC) is present, which in budding yeast is made up of Tof1, Csm3, Mrc1, and Ctf4, to provide structural integrity and confer stability to the fork complex throughout the replication process (reviewed in Baretić *et al.,* 2020).

1.2.3 DDK Complex

It has been established that DDK phosphorylates subunits of the Mcm2-7 complex to initiate DNA replication. Levels of the regulatory subunit, Dbf4, peak at the G1/S phase transition, remaining high throughout the S phase, and ultimately decrease in M-phase due to Dbf4 proteolysis mediated by APC/C (reviewed in Matthews *et al.,* 2012), thereby reducing DDK kinase activity. In contrast, cdc7 levels remain constant throughout the cell cycle (reviewed in Matthews *et al.,* 2012). Dbf4 has three highly conserved motifs: N-terminal (N), medial (M), and C-terminal (C). The N-terminal motif spans amino acid residues 135 – 179 and is necessary and sufficient for Orc2 binding. This region is also required for binding Rad53, which is a protein required in cell cycle checkpoint arrest (further described in *1.2.4 Replication Checkpoint Control of DNA Damage*) (Duncker *et al.,* 2002). Deletion of this region results in slower growth rates under normal replicative conditions. The M motif is necessary for cell viability and maintains binding to replication initiation factor Mcm2 (Varrin *et al.,* 2005). Lastly, the C motif is required for activation of Cdc7, demonstrated by

impaired Mcm2 phosphorylation when essential histidine residues of this region are mutated to alanine (Jones *et al.,* 2010). Crystal structure analysis of the human Dbf4-Cdc7 complex identified binding of Dbf4 to the C- and N-terminus of Cdc7, which acts to tether the complex and activate kinase components, respectively (Hughes *et al.,* 2012).

The preferred target of DDK phosphorylation was initially thought to be Mcm2, but subsequent studies have identified efficient phosphorylation of Mcm4 and Mcm6 as well (Sheu and Stillman, 2010). Furthermore, *in vivo* analysis has revealed that phosphorylation of these subunits is necessary for replication initiation to take place. All other subunits have been shown *in vitro* to be phosphorylated by DDK at lower levels and these additional modifications are not essential for the replication program. The binding of Mcm4 to DDK is specified by a DDK-docking domain ranging from amino acids 175-333 of Mcm4 (Shue and Stillman, 2006). Additionally, a N-terminal Serine/Threonine rich domain (NSD) is present on Mcm4 where phosphorylation by several kinases, including DDK takes place (Sheu and Stillman, 2006). Once phosphorylated by DDK, an inhibitory effect of Mcm2-7 subunits is relieved and allows for further formation of molecular machinery that is responsible for DNA replication, known as the replisome. It was determined that the NSD can be further specified into either a proximal or distal region relative to the DDK-docking domain, which differentially effect origin activation (Sheu and Stillman, 2014). Finally, recent studies have determined that the N-terminal tail of Mcm2 is necessary for DDK binding and phosphorylation of Mcm4, contributing greatly to DDK specificity for Mcm2-7 subunits (Wahab and Remus, 2020).

1.2.4 Replication Checkpoint Control of DNA Damage

As one can imagine, various forms of DNA damage and replicative stress may be introduced throughout the S-phase. This includes exogenous sources such as genotoxic agents or endogenous issues such as the presence of large secondary structures downstream of the replication fork. As a result, *S. cerevisiae* utilizes checkpoint mechanisms, which monitor and act upon any replicative stress that is present. Generally, these systems work by arresting cell cycle progression after detection of DNA damage by sensors, and subsequent transduction of a signal to effector genes which will initiate necessary repair pathways before continuation into the next phase (reviewed in Lirola *et al*., 2008). Ultimately, if the DNA replication stressors cannot be resolved, cells may also induce an apoptosis response. Although checkpoints exist at the G1/S and G2/M phase transitions, I will be discussing the intra-S phase checkpoint as it is most related to the concepts of my project.

When the intra-S DNA checkpoint is activated, replication forks are stalled and firing of remaining late firing origins is downregulated (Zegerman and Diffley, 2010). Although replication forks are stalled, the replicative helicase still unwinds DNA in an uncoupled fashion from the DNA polymerases, resulting in single-stranded DNA (ssDNA) generation. RPAs then binds to ssDNA, which is required to signal for the recruitment of a Mec1 sensor kinase. Within S-phase, this triggers a phosphorylation kinase cascade event through the mediator protein Mrc1, which transmits the signal by scaffolding Rad53 for direct phosphorylation by Mec1. Activated Rad53 then acts as the primary effector that promotes upregulation and recruitment of downstream repair mechanisms, such as upregulation of

deoxynucleotide phosphate (dNTP) production through phosphorylation of the checkpoint kinase Dun1 (Zhao and Rothstein, 2002).

1.2.5 Origin Timing

Even though activated origins are only fired once per genome, there are 352 known origins of replication throughout the budding yeast genome and so there is an organized sequential pattern to firing (Saccharomyces Genome Database, 2021). Origins of replication are fired with different S-phase timings, separated into categories of early, middle, and late firing origins (Raghuraman *et al.,* 2001). Additionally, licensed origins which are unfired during the S phase are considered dormant origins and are thought to serve as a reserve in the event of replicative stress. Specifically, DNA damage may result in stalled forks that can no longer progress or even a complete collapse of a replication fork. Pre-RCs at these dormant origins would then be fired during recovery from these circumstances to ensure complete duplication of the genome (Alver *et al*., 2014). Thus far, the mechanisms that differentiate between origins with respect to replication initiation timing are poorly understood and so several factors are currently being assessed.

One aspect to consider is proteins that distinctly interact with each category of origin to inhibit or promote firing. For instance, the budding yeast protein Rif1, which is involved in telomere length regulation, has been found to inhibit late-firing origins until mid S-phase through dephosphorylation of helicase subunits (Yamazaki *et al.,* 2013). Another factor to consider is the presence of limiting factors which may not be present at every origin when S

phase begins. This would subsequently create origins that fire early and those that fire later dependent on the rate at which replication initiation components are recycled. For example, proportions of Mcm2-7 hexamer recruitment to early and late origins within budding yeast was identified through a single-origin purification method (Das *et al.,* 2015). On average, three MCM complexes were loaded onto a single ARS1 early origin. In contrast, late origin ARS316 loaded less than one MCM on average (Das *et al.*, 2015). Overall, these results speculate that early origins with a higher capacity of MCM complex binding are more likely to fire in comparison to late origins. Additionally, factors that regulate the distribution of these hexamers across the genome is an important aspect to consider. To that end, investigation of Sir2, a gene silencing regulation protein, found that its deletion results in MCM complex accumulation at early origins, with increased replication activity when compared to wildtype budding yeast (Hoggard *et al.*, 2020). Late origin firing was also delayed in this same background, implicating a novel role of Sir2 in maintaining MCM hexamer distribution throughout the genome.

Regarding mammalian studies, more than 60% of origins in human, mouse, and fly cells contain repeated guanine rich segments, termed Origin G-rich Repeated Element (OGRE) (Prorok et al., 2019). Within mouse embryonic stem cells, Prorok and colleagues show that the presence of OGRE motifs affect origin activity, through deletions of these regions causing significantly reduced origin firing. Several methods were employed to verify this finding, including analysis of replication efficiency in a plasmid containing an OGRE insert within a human embryonic kidney cell line (Prorok et al., 2019). Interestingly, these

findings were unexpected as guanine rich regions have been known to impede replisome progression in other organisms, including budding yeast. Specifically, G-quadruplex are secondary structures which can form in presence of repeated guanine stretches and were found to consistently introduce replication instability if left unresolved (Davis and Maizels, 2011). Therefore, it is unclear if repeated guanine rich motifs impede replisome progression through the formation of secondary structures or contribute to a larger role in origin timing regulation.

1.3 Mrc1

1.3.1 Mrc1 Background

Mrc1 is a protein that is involved in several processes within the cell cycle. As mentioned, it is part of a FPC alongside Ctf4, Tof1 and Csm1. The FPC is a component of the replication fork, acting as a structural component to stabilize the associations between DNA and the replisome throughout S phase. A recent study utilizing high resolution electron cryomicroscopy revealed that this FPC resides at the "front face" of the replisome, directly at the junction between polymerase and DNA duplex (Baretić *et al.*, 2020). The FPC also regulates replication rates, demonstrated by increase in replication fork efficiency in the presence of Mrc1 and Tof1 within an *in vitro* replication system (Yeeles *et al.*, 2017).

Another major role of Mrc1 is the transduction of the intra-S phase checkpoint response to facilitate Mec1 phosphorylation of Rad53, as mentioned in the previous subsection. Mrc1 contains 17 SQ/TQ (Serine-Glutamine/Threonine-Glutamine) clusters

primarily located in the medial to C-terminal regions, which are targets of Mec1 kinase activity. The importance of these residues was evident by the 10-fold greater sensitivity to a hydroxyurea (HU) genotoxic stressor in a *mrc1*^{AQ} mutant, where all SQ/TQ motifs are mutated to AQ (Alanine-Glutamine) (Osborn & Elledge, 2003). Furthermore, a study which screened the growth of yeast strains in presence of various Mrc1 truncations genotoxic stressors revealed that the amino acid sequence between 266 and 635 are critical in maintaining the checkpoint response of Mrc1 to replicative stress (Naylor *et al*., 2009). The presence of the three SQ/TQ motifs in this region are necessary for a functional checkpoint response. Despite the small number of SQ/TQ motifs in this region, mutations at those regions consistently delayed Rad53 activation timing and intensity. Mrc1-C14 (amino acid residues 1–843) and Mrc1-N4 (amino acid residues 266–1096) were the largest truncations at each terminal end of Mrc1 that still conferred HU resistance to levels of wildtype cells (Naylor *et al*., 2009). Therefore, the phosphorylation activity of various SQ/TQ motifs distributed throughout the Mrc1 sequence are important in maintaining its checkpoint response function.

Rad9 is another mediator with a redundant role of transducing a kinase cascade signal from Mec1 during a checkpoint response. Mrc1 is the primary mediator during the intra-S phase checkpoint response and Rad9 is the primary mediator for DNA damage responses at other stages of the cell cycle. However, cooperative interplay between Mrc1 and Rad9 has been investigated recently, revealing distinct mechanisms that complement each other. First Mrc1 activated Rad53 at stalled replication forks, to induce late origin firing suppression.

Overtime, Mrc1 signaling is reduced and Rad9 is recruited to sustain checkpoint activity of Rad53 (Bacal *et al.*, 2018).

With roles as a mediator of checkpoint responses and fork protection, Mrc1 interacts with many proteins and is difficult to purify in high concentrations for structural analysis. However, the three-dimensional structure of Mrc1 was recently discovered to be a ring, in a nearly circular conformation based upon electron microscopy reconstitution techniques (Li & Zhang, 2020). Furthermore, this study revealed that DNA passes through the center hole of the circular Mrc1 structure, based upon DNA density analysis of these 3D reconstructions. This is consistent with previous findings that human Claspin forms a ring and binds with high affinity to single-stranded DNA (Sar *et al*., 2004).

1.3.2 Checkpoint-Independent Role of Mrc1 at Early Origins of Replication

In the past decade, studies have implicated a potential role of Mrc1 in the regulation of origin firing through interactions with DDK. Mrc1 is required for efficient scaling of DNA replication in budding yeast, with slow fork progression and an extended S-phase in a ΔMrc1 background (Koren *et al*., 2010). The checkpoint function of Mrc1 was not required to maintain scaling, revealing a potential role of Mrc1 in normal DNA replication conditions.

Mrc1 binds to and associates with early origins in a checkpoint-independent manner to regulate their firing in *Schizosaccharomyces pombe* (fission yeast) (Masai *et al.,* 2017). This regulation of early origin firing is proposed to occur in a checkpoint-independent manner. This was initially based upon the finding that early origin firing was increased in

Δ*mrc1* fission yeast cells when compared to both wildtype cells and $mrc1^{AQ}$ mutants (Hayano *et al.*, 2011). Recently, a model detailing origin firing regulation by Mrc1 and Hsk1 (Cdc7 homologue in fission yeast) has been developed. Matsumoto and colleagues propose that Mrc1 exists in either a "break-on" or "break-off" conformation (Masai *et al.*, 2017). Prior to replication initiation, Mrc1 is selectively bound to early origins in the "break-on" conformation through intramolecular interactions between a 98 amino acid C-terminal Hsk1 bypass segment (HBS) and the N-terminal target of HBS (NTHBS) region. When maintained in this conformation, early origin firing is downregulated. As S phase begins, Hsk1-Dfb1 (budding yeast Cdc7-Dbf4 ortholog) is recruited to Mrc1 at the site of the intramolecular interaction, phosphorylating an adjacent region, converting Mrc1 to the "break-off" conformation which induces early origin firing. Besides the proposed fission yeast model, Cdc7 was found to phosphorylate and interact with Claspin (vertebrate homologue of Mrc1) within HeLa human cells (Kim *et al.*, 2008). *In vitro* analysis of *Xenopus* egg extracts also demonstrates evidence of nuclear complex formation between DDK and Claspin (Gold & Dunphy, 2010).

Within *S. cerevisiae*, Mrc1 has been found to interact with early and late origins with distinct timings. Chromatin immunoprecipitation (ChIP) assays have been conducted to assess Mrc1 binding to known origins. Strains with epitope tagged Mrc1 cells were released from G1 cell cycle arrest at 19 °C to slow fork movement and it was found to periodically associate with various genomic loci. Consistently, Mrc1 bound to early origin ARS305 faster from release, whereas association with the late origin ARS603 displayed significantly

delayed kinetics (Osborn & Elledge, 2003). Furthermore, this association with ARS305 was DDK-dependent, as Mrc1 binding to this origin diminishes when DDK activity is downregulated (Osborn & Elledge, 2003).

1.4 Research Objectives

Details of Mrc1 as a novel regulator of replication initiation have been introduced in fission yeast, providing insight towards a Mrc1-Hsk1 based model at early origins. However, the interaction between DDK and Mrc1 has not been well characterized in budding yeast thus far. The goal of my thesis is to utilize *Saccharomyces cerevisiae* to further characterize the interactions between Mrc1 and DDK and to use these findings to develop a better understanding of origin timing regulation. Specific objectives to reach this goal included:

1. Determine the minimum region of Mrc1 required to facilitate an interaction with DDK, by carrying out a series of Y2H assays with specific regions of Mrc1, dividing the protein into progressively smaller portions and assessing interactions with DDK subunits.
2. Create a Mrc1 mutant strain which lacks the DDK interacting domain. Conduct a growth curve assay to evaluate the phenotype and potential checkpoint-independent function of this mutant strain in budding yeast.
3. Confirm checkpoint function of this Mrc1 mutant strain, to ensure that any differential growth phenotype is not due to a nonfunctional response to replicative stressors. If successful, this will create a separation of function as the speculative role of Mrc1 in DNA replication initiation may be affected in this mutant, but the checkpoint response is

retained. This will be assessed through genotoxic spot plate assays, to determine growth in the presence of DNA damaging agents.

4. Evaluate the effect of the separation of function Mrc1 mutant on DNA replication progression and loading of the Mrc1 mutant onto early origins during DNA replication initiation through Fluorescence-Activated Cell Sorting (FACS), plasmid stability assays, and Chromatin Immunoprecipitation (ChIP).

1.5 Significance of Research

Several studies have demonstrated elevated levels of human DDK in tumor cell lines due to an overexpression of each subunit. This overexpression of DDK is correlated with advanced tumor grade is multiple cancers, such as breast and ovarian cancer (Sasi *et al.*, 2017). Cdc7 depletion in HeLa cells also consistently inhibited DNA replication, eventually leading to cell apoptosis without the activation of any cell cycle checkpoint response (Montagnoli *et al.*, 2004). These findings are not all that surprising considering DDK is an essential component that is directly proportional to origin firing. Therefore, the study of how Mrc1 interacts with DDK to potentially regulate DNA replication initiation is of significant value. In a practical sense, findings that may downregulate DDK expression or recruitment in these cells can be directly applied to cancer therapeutics and medical applications in the future. If the current model is accurate, then upregulation of Dbf4 is associated with enhanced origin firing, which would support the increase in DNA replication in cancer cell lines (Masai *et al.*, 2017). If a Mrc1-DDK based regulation of origin firing can be further

characterized in budding yeast, the fundamental pathway can be explored in greater complexity with the Mrc1 human homologue, Claspin.

Chapter 2: Materials and Methods

2.1 Yeast Strains

Yeast strains outlined in the following table were utilized for yeast two-hybrid, spot plate, growth curve, FACS, and ChIP assays (Table 2.1). Specific strains used in each assay will be outlined in throughout various sections in chapter 2.

Table 2.1 Yeast Strains Used in this Study

Strain	Genotype	Source
DY-1	*MATa, ade2-1, can1-100, trp1-1, his3-11, ura3-1, leu2-3, leu2-112, pep4::LEU2*	Duncker *et al.,* 2002
DY-30	*MATa, his3Δ1, leu2Δ0, met15Δ0, ura3Δ0*	Brachmann *et al.,* 1998
DY-81	*MATa, ade2-1, can1-100, trp1-1, his3-11, his3-15, ura3-1, leu2-3, leu2-112, pep4::LEU2, orc2::ORC2myc13-TRP1*	Ramer, 2011
DY-147	*MATa, ade2-1, can1-100, his3-11,15, leu2-3, trp1-1, ura3-1, SML1::HIS3, RAD5, RAD53::URA3*	Tam *et al.,* 2008
DY-298	*MATa hisD1, leu2D0, met15D0, ura3D0, Mrc1::KanMX*	Open Biosystems
DY-391	*MATa hisD1, leu2D0, met15D0, ura3D0 Mrc1::Mrc1ΔN1.1*	This study
DY-394	*MATa hisD1, leu2D0, met15D0, ura3D0 Mrc1::Mrc1-Myc1-HIS3MX6*	This study
DY-395	*MATa hisD1, leu2D0, met15D0, ura3D0 Mrc1::Mrc1ΔN1.1-Myc1-HIS3MX6*	This study

N1.1 refers to the N-terminal amino acids 1-186 region of wildtype Mrc1. Deletion of this region in the DY-391 strain was introduced using a two-step gene modification system called *delitto perfetto* (Storici *et al.,* 2006). The first step involved the amplification of a

URA3 cassette from a pRS406 vector, which was integrated through homologous recombination at the MRC1N1.1 locus (Sikorski & Hieter, 1989). These cells were then grown on synthetic complete medium lacking uracil to select for the disrupted MRC1 strain. In step two, a replacement cassette containing the modified Mrc1ΔN1.1 sequence and two 60 nucleotide homologous flanking regions was transformed into cells and plated on YPD. Finally, replica plating of colonies onto 5-Fluoroorotic acid containing media selected for cells that have lost the intermediate URA3 cassette and have successful Mrc1ΔN1.1 genomic integration. Genomic DNA from candidate colonies was isolated and submitted for sequencing at SickKids TCAG Facilities. Mrc1-Myc1 (DY-394) and Mrc1ΔN1.1-Myc1 (DY-395) strains were created from DY-30 and DY-391, respectively. *Myc* tagging was completed using a Polymerase Chain Reaction (PCR) based gene modification strategy (Longtine *et al.,* 1998). Primers were designed to amplify a 13Myc-HIS3MX6 cassette from a pFA6A derived vector. The primers used to amplify this cassette also contained flanking sequence ends that were complementary to the C-terminal encoding region of *MRC1* for tagging. Specifically, the forward primer contained sequences complementary to a 400bp region upstream of the Mrc1 stop codon. The reverse primer contained sequences complementary to the 3' untranslated region directly downstream from the stop codon. This amplification product was then transformed into either a wildtype Mrc1 (DY-30) or Mrc1ΔN1.1 (DY-391) background strain and homologous recombination of the flanking ends resulted in C-terminal tagged proteins. Genomic DNA was isolated from colonies grown on synthetic complete plates lacking histidine (SC-His). Genomic DNA from candidate colonies were isolated and a PCR was conducted using a primer pair that confirms

the presence of a Myc-tag. This amplified product was finally submitted to SickKids TCAG Facilities for sequencing.

2.2 Plasmid Construction

Various yeast two-hybrid plasmid constructs containing specific regions of Mrc1 were generated in this study using similar yeast cloning techniques (each construct is specified in section 2.4: *Yeast Two-Hybrid Assay*). pEG202 and pJG4-6 two-hybrid plasmid vectors were used as the backbone for cloning (Ausubel et al., 1994; Gyuris et al., 1993). Each region of Mrc1 was first amplified from DY-1 genomic DNA through PCR. The primers used for PCR contained BamHI and Xho1 restriction sites on the forward and reverse primers, respectively. The PCR product and two-hybrid vector of interest were then restriction digested by both enzymes (Thermo Fisher Scientific), followed by PCR cleanup using a commercial kit (Geneaid). T4 DNA ligation was completed using a commercial kit (BioBasic) and the products were transformed into calcium-chloride competent Escherichia coli cells. Potential clones were then grown on Lysogeny broth (LB) media containing 100 µg/ml ampicillin because each two-hybrid vector contains an AmpR gene which confers ampicillin resistance through β-lactamase enzyme production. Finally, colony PCR was conducted using a commercial kit (New England Biolabs) and colonies with amplification of the target DNA length were grown to saturation (1×10^8 cells/ml) in LB + Ampicillin media. Forward primers were designed with specificity to the vector sequence directly upstream from the cloning site (either pEG202 or pJG4-6). Reverse primers were designed with

specificity to the specific region of *MRC1* of that was cloned. Plasmid preparations were made using a commercial kit (Geneaid) and several clones were sent for sequencing at SickKids TCAG Facilities.

2.3 Yeast Transformation

Yeast strains to be transformed were grown to saturation, followed by growth to a working concentration of 1 x 10^7 cells/ml in 10 ml of appropriate media. Either general growth YPD medium or various selective synthetic complete media were used depending upon the genotype of the strain or previous plasmid transformations. Working cultures were centrifuged for 5 minutes at 4000 rotations per minute (rpm) and resuspended in 10 ml of sterile 1X Tris-EDTA (TE) pH 8.0 buffer. Cells were centrifuged again, resuspended in 2 ml 100mM lithium acetate (LiAc)/0.5x TE solution, and incubated at room temperature for 10 minutes to create a yeast suspension mix. A portion of the yeast suspension mix (100 µl) was added to a sterile 1.5 ml tube alongside 0.4-0.6 µg plasmid DNA of interest and 100 µg of salmon sperm DNA (Thermo Fisher Scientific). A LiAc/40% polyethylene glycol 4000/1x TE solution (300 µL; 100mM) was then added and incubated for 30 minutes at 30°C. Dimethylsulfoxide (40 µl) was added, and each tube was incubated at 42˚C for 7 minutes. Following immediate cooling on ice for 2 minutes, contents of each tube were plated on individual selective media and grown for 2 – 3 days at 30°C.

2.4 Yeast Two-Hybrid

DY-1 yeast cells were first transformed with a pSH18-34 lacZ reporter plasmid, followed by co-transformation of pEG202 and pJG4-6 derived vectors (Ausubel et al., 1994). For this study, pEG202 derived vectors were constructed with specific regions of wildtype MRC1, termed "bait" constructs. Each region of MRC1 that was cloned into pEG202 (using previous outlined techniques in 2.2: Plasmid Construction) are outlined in figure 2.1.

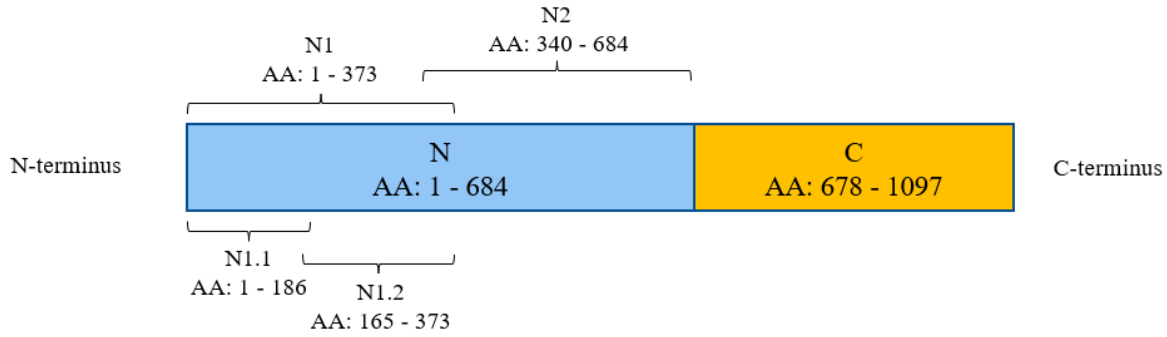

Figure 2.1 Mrc1 Regions cloned into pEG202 for Yeast Two-Hybrid. Several yeast two-hybrid trials were conducted with pEG202 derived "bait" vectors that contained specific regions of Mrc1. Mrc1 is 1096 amino acids in length. The various Mrc1 subsections are outlined alongside the associated amino acid ranges.

pJG4-6 derived vectors were constructed with wildtype DBF4 sequence. A culture containing triple transformants were selected for in 10 ml of synthetic complete media lacking uracil, tryptophan, and histidine (SC-UTH), grown to $1x10^7$ cells/ml. Cells were then washed in water and induced in 20 ml 2% Galactose-1% Raffinose media lacking uracil, tryptophan, and histidine for 6 hours to promote the expression of the prey protein. Expression is induced due to a GAL1 promoter, which is activated in the presence of galactose and repressed in its absence. Following the induction period, 5×10^6 cells/ml were

harvested and subjected to yeast two-hybrid assay including determination of β-galactosidase activity. Cells were centrifuged at 16,000 x g for 10 minutes and resuspended in 0.5 ml Z buffer (60 mM Na2HPO4, 40 mM NaH2PO4, 10 mM KCl, and 1 mM MgSO4). Two drops of chloroform and 1 drop of 0.1% SDS were added to each tube and vortexed for 10 seconds at maximum speed. Samples were incubated at 28˚C for 5 minutes, followed by the addition of 100 µl 4 mg/ml ortho-Nitophenyl-ß-galatoside (ONPG).

Sequences encoding a LexA DNA binding domain and a B42 transcriptional activation domain are fused to the genes of interest expressed in the bait and prey vector, respectively. If there are physical interactions between these proteins, these two domains will be in close proximity to form an active transcription factor that will stimulate β-galactosidase production through activation of 8 LexA operators which regulate LacZ reporter gene expression. ONPG is normally a colorless compound, however, β-galactosidase hydrolyzes it to form ortho-nitrophenyl (ONP), a yellow colorimetric compound. Once one of the samples has developed a pale yellow colour following ONPG addition, all the reactions are stopped with the addition of 250µl of 1M Na2CO3 to each tube. Cell debris is centrifuged at 16,000 x g for 10 minutes and the intensity of yellow color supernatant in each sample was measured at 420 nm (A420). β-galactosidase of each sample was calculated using the following formula: β-galactosidase activity units = 1000 x A420/ (t x v x A600), where A420 is the absorbance of the ONP product, A600 is the cellular density of the culture, t is the time elapsed from the addition of ONPG until the addition of 1M Na_2CO_3, and v is the volume of culture added in ml for 5 x 10^6 cells.

2.5 Whole Cell Extract and Western Blot

20 ml of working yeast culture ($1x10^7$ cells/ml) was centrifuged at 4000 rpm for 5 minutes. Pellets were washed once with sterile water, centrifuged once again, and resuspended with 400 µl of lysis buffer (ice-cold and prepared fresh; 50 mM HEPES-KOH pH 7.5, 140 mM NaCl, 1 mM EDTA, 1% Triton X-100, 0.1% Na-deoxycholate, 1% PMSF, 1% protease inhibitor cocktail Fisher). Samples were then transferred into 2 ml screw cap tubes that contained 0.3g of 0.5mm glass beads. Next, samples were stored on ice and transferred to a 4°C walk-in incubator Mini Beadbeater (BioSpec Products). Cells were lysed in 8 cycles, alternating between 30 seconds of bead beating followed by 30 seconds of rest on ice. Each tube was centrifuged at 13,200 rpm for 30 seconds at 4°C. The supernatant was separated from cellular debris and beads into a new 1.5 ml tube, at which point 4 µl of each sample was aliquoted and set aside for a Bradford assay to determine protein concentration in each sample (BioRad Protein Assay Dye). Freshly prepared 4X loading dye (41.5 mM Tris pH 6.8, 10% glycerol, 3.75% SDS, 0.01% bromophenol blue, 100 mM dithiothreitol; 50 µl) was added to 100 µl of supernatant sample in a new 1.5 ml tube. Samples were denatured by incubation at 95°C for 10 minutes.

80 µg of each sample and 5 µl of protein ladder (FroggaBio) were loaded onto a 10% polyacrylamide gel and SDS polyacrylamide gel electrophoresis (SDS-PAGE) was conducted until desired separation based upon size of proteins of interest. The protein ladder contained 12 pre-stained proteins spanning molecular weights from 11 to 245 kilodalton (kDa), which is included to estimate the size of migrated proteins after sufficient separation.

The polyacrylamide gel was transferred onto a nitrocellulose membrane and placed into a cassette containing Whatman paper and sponges. Transfer buffer (200 mM glycine, 25 mM tris-base, 20% methanol, 0.05% SDS) was added until the cassette was completely submerged, and samples were transferred overnight (OWL transfer system) at 4^{o}C. Membranes were stained with 0.1% Ponceau S, to verify consistent transfer of proteins, and de-stained with 1X TENT (20 mM Tris-HCl, 1 mM EDTA, 150 mM NaCl, 0.1% Tween 20). Membranes were then submerged in a skim milk solution (1X TEN + 5% skim milk powder) as a blocking buffer for 1 hour with gentle shaking at room temperature. The blocking solution was then removed, and the membrane was washed with 1x TENT for 5 minutes. This was followed by primary antibody incubation for 2 hours at room temperature with gentle shaking. A wash step was then completed 3 more times with 1X TENT, followed by 1 hour of incubation in the dark with secondary antibodies. A final 1X TENT wash step was completed, and membranes were imaged using an imager (Pharos FX Plus). Antibodies used in this study are outlined in the table below (table 2.2).

Table 2.2 Antibodies Used in Study

Antibody	Antibody Type	Dilution	Source
Anti-HA: mouse monoclonal	Primary	1:5000 in 3% BSA	Sigma
Anti-LexA: rabbit polyclonal	Primary	1:5000 in 3% BSA	ABR
AlexaFlour 647: goat anti-rabbit	Secondary	1:3000 in 5% skim milk solution	Invitrogen
AlexaFlour 488: goat anti-mouse	Secondary	1:3000 in 5% skim milk solution	Invitrogen
Anti-Myc: mouse monoclonal	Primary	1:5000 in 3% BSA	Sigma

2.6 Growth Curve and Spot Plate Assay

Growth Curves for Mrc1 mutant strains were completed by growing each culture to a concentration of $5x10^{6}$ cells/ml in 10 ml YPD liquid media. Cultures when then diluted to a starting concentration of 5×10^{5} cells/ml and were grown at 30ºC in YPD for a total of 12 hours. Cell concentration was determined every two hours using a light microscope and a hemocytometer, for a total of 7 data points for each strain. The final growth curve is an average of three independent trials.

The spot plate assay was conducted using YPD media both with and without the presence of genotoxic agents. Trials completed to assess Mrc1ΔN1.1 strain (DY-391) growth were conducted alongside a ΔMrc1 mutant (DY-298) and WT Mrc1 (DY-30) strain for direct comparison. Additionally, a ΔRad53 strain (DY-147) was used because Rad53 is a DNA

damage kinase that is required to maintain checkpoint control. Therefore, the ΔRad53 strain is expected to have little to no growth on plates in the presence of genotoxic stressors and will act as a control to ensure effectiveness of each additive. Yeast cultures were grown to saturation and then serially diluted ten-fold 4 times using a sterile 60-well plate. A multichannel pipettor was then used to pipette 5 µl of each dilution onto the appropriate plate, which were grown for 48 hours at 30ºC and imaged (ChemiDoc MP; BioRad).

2.7 Fluorescence-Activated Cell Sorting (FACS)

FACS analysis was completed for Mrc1ΔN1.1 (DY-391), ΔMrc1 (DY-298), and WT Mrc1 (DY-30) strains. Yeast cultures were grown to a working concentration of $1x10^7$ cells/ml in 10 ml YPD media. 1×10^8 cells from each sample were transferred to 20 ml fresh media and centrifuged for 4 minutes at 6000 x G. This media was decanted, and the pellet was washed in 20 ml sterile water, centrifuged once again, and resuspended in 30°C preheated YPD media containing 40 µg/ml α-factor. Cultures were incubated for 2.5 hours at 30°C to induce cell cycle arrest in G1 phase, which was verified under a light microscope by the pear shape "schmoo" morphology. Following verification of arrest, cells were spun down for 4 minutes at 6000 x g and washed 2 times in 20 ml sterile water as described previously. YPD containing 50 µg/ml pronase E was then used to degrade any remaining α-factor and induce release from checkpoint arrest. Samples were collected at regular 10-minute intervals from timepoint 0 – 40 minutes, totaling to 5 timepoints. Aliquots of timepoints 10 and 20 minutes were taken for observation under light microscopy to verify budding of yeast cells

due to release from cell cycle arrest. A each timepoint, 1.5 ml of each culture (at 7 x 10^6 cells/ml) was transferred into a 1.5 ml tube and centrifuged at 13,000 rpm for 1 minute. The pellet was then resuspended in 1 ml of 70% ethanol and stored at 4°C until further sample preparation. A portion of each sample (500 µl) was transferred into a new 1.5 ml tube, centrifuged once again, and the pellet was resuspended in 500 µl dH_2O. Cells were then treated with 500 µl of 10mg/ml RNase.

Cells were then resuspended in 500 µl proteinase K solution (2 mg/ml in 50 mM Tris-HCl) for 45 minutes at 50°C. Following another centrifugation, the pellet was resuspended in 100 µL of FACS buffer (200 mM Tris-HCl pH 7.5, 200 mM NaCl, 78 mM MgCl2) and transferred to a 5 ml Falcon tube containing 750 µL Sytox solution (50mM Tris-HCl pH 7.5, 1:5000 dilution 5mM Sytox solution in Dimethylsulfoxide [Molecular Probes #S-7020]). Finally, cells were sonicated for 5 seconds at low intensity just prior to FACS analysis using Amnis ImageStream Flow Cytometry.

2.8 Chromatin Immunoprecipitation (ChIP)

ChIP protocol was modified based upon Matthew D. Ramer, 2011. Yeast working cultures were grown in 50 ml of YPD (1.5x10^7 cells/ml) within a 250 ml Erlenmeyer flask, followed by protein cross-linking with 1% formaldehyde for 20 minutes at 30ºC with gentle shaking. The reaction was quenched by the addition of 2.5 ml of 2.5 M glycine and incubation for 5 minutes at 30ºC without shaking. Cultures were centrifuged at 4000 rpm for 5 minutes and pellets washed once with 40 ml of ice-cold Phosphate-buffered saline (PBS).

Cells were pelleted and resuspended in 400 µl lysis buffer (10mM Tris-HCl, 50 mM HEPES-KOH pH 7.5, 140 mM NaCl, 1 mM EDTA, 1% Triton X-100, 0.1% Na-deoxycholate, 1% PMSF, 1% protease inhibitor cocktail Fisher). Each sample was transferred to a 2 ml screwcap tube filled with 0.3g of 0.5 mm glass beads and lysed in a Mini Beadbeater at 4ºC for 8 cycles, alternating between 30 seconds of lysing and 30 seconds of rest on ice. Each tube was centrifuged at 1000 x g for 30 seconds to separate glass beads and cell debris in the pellet from the cell lysate supernatant. This supernatant was then transferred to a new 1.5 ml tube and centrifuged at 16,000 x g for 5 minutes. The supernatant was discarded, and the final pellet was resuspended in 500 µL of lysis buffer. The intensity dial of the sonicator (Ultrasonix) was set to 4, to achieve a reading of 5-6 watts on the display. All samples were sonicated for 6 cycles, alternating between 20 seconds of sonication and 2-minute rest on rice. Samples were centrifuged at 4500 x g for 2 minutes and the supernatant was transferred to a new 1.5 ml tube. This centrifugation step was completed twice, and the supernatants were pooled to form the whole cell extract (WCE) sample. A portion of each WCE extract (25 µl) was placed in a new 1.5 ml tube as the INPUT (IN; stored at -20°C). Remaining volumes of all WCE samples were added to a new 1.5 ml tube containing 40 µl of 10 mg⁄ml magnetic Dynabeads (sheep anti-mouse IgG; M-280 Dynal Biotech) previously incubated with anti-Myc antibody (Sigma #M5546).

Bead preparation was completed one day before incubation with WCE. Dynabeads (40 µl) were washed 5x with 200 ml PBS +BSA (5mg/ml), using a magnetic particle concentrator (MPC) to pull down beads. After the final wash, magnetic beads were

resuspended in 40 µl of the same PBS+BSA solution. Anti-Myc antibody (3 µl) was then added to each tube and incubated overnight with rotation at 4°C. A portion of each sample (30 µl) was transferred to a fresh 1.5 ml tube, a MPC was then used to remove liquid, and the WCE was added to the magnetic beads. Once again, each sample was incubated on a rotator at 4°C overnight. The following day, magnetic beads were pulled down with the MPC and the supernatant was transferred to a fresh tube and stored at -20°C. The beads were then incubated with lysis buffers containing varying NaCl concentrations, washed with a wash buffer, and finally incubated in 1x TE. Each step was completed for 5 minutes with rotation and separated using a MPC in the following order:

1. 2x 600 µl lysis buffer (50 mM HEPES-KOH pH 7.5, 140 mM NaCl, 1 mM EDTA, 1% Triton X-100, 0.1% Na-deoxycholate, 1% PMSF, 1% protease inhibitor cocktail Fisher)
2. 2x 600 µl lysis buffer (50 mM HEPES-KOH pH 7.5, 400 mM NaCl, 1 mM EDTA, 1% Triton X-100, 0.1% Na-deoxycholate, 1% PMSF, 1% protease inhibitor cocktail Fisher)
3. 2x 600 µl wash buffer (10mM Tris-HCl pH 8, 250 mM LiCl, 1mM EDTA, 0.5% NP-40, 0.5% Na-deoxycholate)
4. 1x 600 µl TE pH 8

60 µl elution buffer (10mM Tris-HCl, 1mM EDTA, 1% SDS) was added to each sample and incubated at 65 °C for 10 minutes, with gentle mixing every 2 minutes. This step was completed twice and the supernatant, now the immunoprecipitate (IP), was transferred into a new 1.5 ml tube. Formaldehyde crosslinks were reversed through incubation of both IP and IN samples at 65 °C for 8 hours. Following crosslink reversal, IP samples were incubated for

2 hours at 37 °C with the addition of 240 µl TE, 4 µl glycogen (10 mg/ml), and 10 µl Proteinase K (20 mg/ml). Half of these amounts were added to the IN samples.

Next, 50 µl and 25 µl of 5 M LiCl were added to the IP and IN samples, respectively. 564 µl and 282 µl Phenol:chloroform:isoamylalcohol (25:24:1 ratio) was added to IP and IN samples, respectively. Each sample was vortexed until a milky appearance was observed and centrifuged at 16,000 x g for 2 minutes at room temperature. The aqueous layer was retained and a 2x volume of 100% EtOH was added before DNA precipitation overnight at -20°C (IP =1128 µl and IN = 564 µl of 100% EtOH added). Samples were then centrifuged at 16,000 x G for 10 minutes in the cold room and the pellet was washed with a half volume of ice-cold 70% EtOH (IP =564 µl and IN = 282 µl of 70% EtOH added). Samples were centrifuged for 5 minutes at 16,000 x G and EtOH was removed carefully using a P20 micropipette, to avoid dislodging the DNA pellet. Finally, all samples were resuspended in 60 µl TE. ChIP PCR for this study was optimized with the following cycles for amplification of ARS305:

1. 95.0 °C for 5 minutes
2. 95.0 °C for 1 minute
3. 55.0 °C for 1 minute
4. 72 °C for 1 minute
5. 45X repetition of steps 2 to 4
6. 72 °C for 7 minutes

ARS305 primers were designed based upon ChIP experiments in Osbourne and Elledge, 2003. ARS305 specific forward primer = (GATTGAGGCCACAGCAAGACCG) and ARS305 specific reverse primers = (CTCCGTTTTTAGCCCCCCGTG) (Osbourne and Elledge, 2003).

Amplification of this region resulted in a 280 base pair fragment. The PCR reaction mix contained 3 μl IN and 5 μl IP as templates. In addition to the amplification of ARS305 specific regions, a control primer pair was also designed to amplify non-origin regions 8kb upstream of the target site. The resulting 361 base pair region is amplified by ARS305 8kb upstream forward primer = (CCGCAAAAGCGGGTTACCCA) and ARS305 8kb upstream reverse primer = (GACAGGACAGAGTTTGGATGCAAC). An 8kb downstream region control primer set was also utilized to generate a 174 base pair amplified region. For this, ARS305 8kb downstream forward primer = (GGTGGTGGAGAAGCGGTTCAAAG) and ARS305 8kb downstream reverse primer = (GCCCTTTGGAGACTGAGAAGGC) were utilized. PCRs of all three regions were completed together and ran on a 2% agarose gel at 80V for 1.5 hours and visualized using an imager (ChemiDoc MP; BioRad).

2.9 Plasmid Stability and Loss Assay

Strains of interest were first transformed with a YCplac111 plasmid and grown for selection on SC-leu media plates using techniques previously described (Gietz & Sugino, 1988). One colony per strain was picked and grown to saturation in SC-leu liquid media. A portion of cells ($2x10^3$) were inoculated into 10 ml SC liquid media, containing leucine, and grown to saturation once again. A light microscope and hemocytometer were used to count cells and plate approximately 400 cells onto 10 SC-leu and 10 SC complete media plates. The final counts from the 20 total plates per strain were used to represent a percentage of

plasmid loss. Plasmid loss per generation was calculated as (1- (colony number on SC-leu/colony number on YPD))/number of cell divisions.

Chapter 3: Mrc1 N-terminus Mediates Interactions with Dbf4, Promoting Optimal Growth Rates in a Checkpoint-Independent Fashion

3.1 Introduction

The sequential firing of origins throughout S-phase, or origin timing, is an important feature to ensure temporal firing of the 352 known origins, in an organized manner (Saccharomyces Genome Database, 2021). However, the mechanisms which differentiate between early and late firing origins are not well characterized. One possibility previously discussed may be the availability of limiting factors, such as Dbf4, which are required for origin firing. Dbf4 is not incorporated into the final replisome structure and instead phosphorylates Mcm2-7 subunits for recruitment of downstream replication initiation factors. As a result, the abundance of Dbf4 at origin sites is very low and this regulatory subunit is not available at every single firing origin (Mantiero *et al.,* 2011). Instead, it is sequentially loaded with initial enrichment at early origin sites for phosphorylation, followed by dissociation, and final reassociation at late origins as S-phase progresses. As an essential component of replication initiation, variable recruitment of these limited factors to specific origins is a notable difference between early and late firing origins. Similarly, Rif1 accumulates specifically at late origins and acts as an inhibitory factor to delay origin firing (Yamazaki *et al.,* 2013).

As mentioned previously, the interaction between DDK and Mrc1 has not been well characterized in budding yeast, especially as it pertains to a potential checkpoint-independent function. Mrc1 is known to bind to early origin ARS305 consistently earlier than late origin ARS603 in *S. cerevisiae*, indicating a potential role in sequential firing of these origins (Osborn & Elledge, 2003). Furthermore, studies in fission yeast have extended this area of

study with the proposal of Mrc1 regulated early origin firing through the recruitment of Hsk1 (budding yeast Cdc7 equivalent) to a site of intramolecular interactions. Specifically, Hsk1 is recruited to the site of interaction between C-terminal Hsk1-bypass segment (HBS) and N-terminal target of HBS (NTHBS) regions of Mrc1 (reviewed in Masai *et al.,* 2017). Following Hsk1 recruitment, a N-terminal region of Mrc1 is phosphorylated to disrupt the intramolecular interaction within Mrc1 and increase origin firing efficiency. Deletions of the intramolecular interacting domains prevents Hsk1 recruitment and facilitates dissociation of intermolecular interactions to promote increased origin firing rates. These findings support a checkpoint-independent role of Mrc1 as DNA replication rates in the absence of replication stressors is directly affected by the conformation of Mrc1, following DDK interactions. Evidence of a similar mechanism has been implicated in other eukaryotes, such as the N-terminal region of Claspin (budding yeast Mrc1 equivalent) interacting with an acidic patch on its own C-terminus in 293T cells (Yang *et al.,* 2016). Claspin was also found to phosphorylate and interact with Cdc7 based upon coimmunoprecipitation findings in HeLa cells (Kim *et al*., 2008). Overall, a checkpoint-independent role of Mrc1 has been implicated in other eukaryotes and is an area of research in budding yeast to be explored further.

Initial Y2H trials completed by Larasati and Celine Aziz in the Duncker lab investigated which subunit of DDK, Cdc7 or Dbf4, interacts with Mrc1. Preliminary data showed that that there was a strong interaction between Mrc1 and Dbf4 (Figure 3.1; reproduced with permission from Larasati, 2020). Conversely, Mrc1 binding to Cdc7 was very low, like that of negative control samples which lack either a bait or prey Y2H vector.

These initial results contrast those that were found in fission yeast and indicate that budding yeast Mrc1 may not regulate origin timing control in the same manner. As a result, initial goals were to verify these findings and further characterize a discrete binding region between Mrc1 and Dbf4.

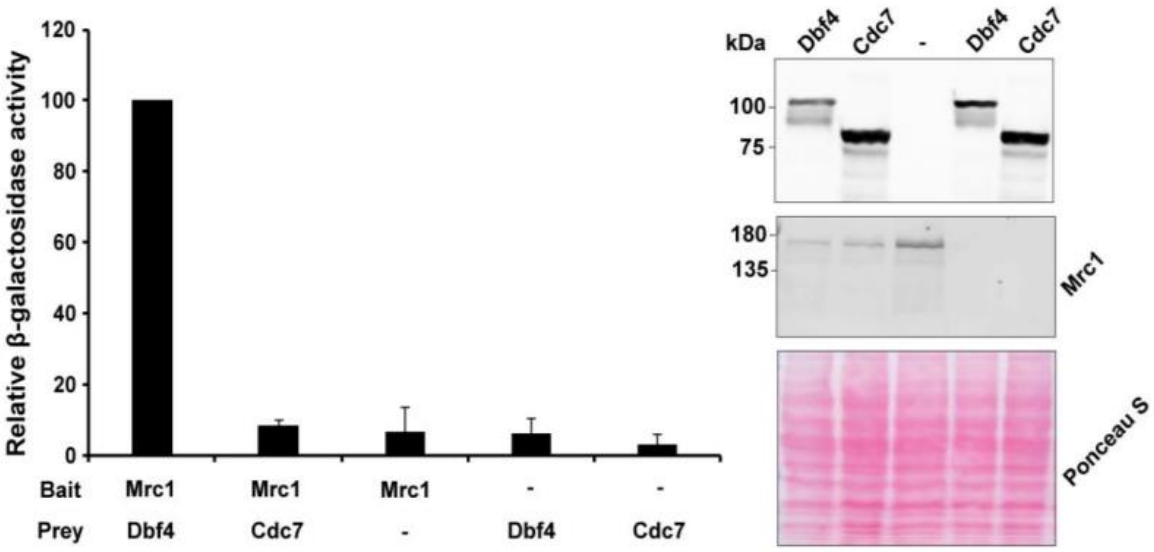

Figure 3.1 Mrc1 binds to Dbf4, not Cdc7. Yeast two-hybrid results are presented as a percentage of β-galactosidase activity in the Mrc1-Dbf4 trials. pEG202 and pJG4-6 were used as bait and prey vectors, respectively. Each interaction was evaluated in triplicate independent trials and error bars represent standard deviation. Anti-LexA and anti-HA was used to detect proteins expressed in bait and prey vectors, respectively. Ponceau S staining shows consistent protein loading in each lane. Trials including empty bait or prey vectors were included as controls for β-galactosidase activity and western blotting (Figure reproduced with permission from Larasati, 2020).

Mrc1 multiple Sequence alignments amongst various fungal species, performed by Larasati and Zohaib Merali from the Duncker lab, revealed that the binding domain of Hsk1 at the site of Mrc1 intramolecular interactions in fission yeast is not well conserved (Larasati,

2020). However, the C-terminal region of Mrc1 is known to contain acidic patches, which have been well characterized to mediate protein-protein interactions amongst other proteins in yeast (Hodges *et al.*, 2017). Specifically, three distinct amino acid patches were identified: 720 – 729, 808 – 813, 813 – 986 (Larasati, 2020). Y2H trials were completed by Larasati with separate bait vectors containing "Mrc1 N", spanning amino acid residues 1 – 684, and "Mrc1 C", spanning amino acid residues 679 – 1096 (Figure 3.2; reproduced with permission from Larasati, 2020). These results indicated that the N-terminal region of Mrc1 was responsible for mediating interactions with Dbf4, not the C-terminal end. Interestingly, Mrc1 N-Dbf4 Y2H trials showed higher β-galactosidase activity in comparison to full length Mrc1. This may be due to the N-terminal truncation allowing for the interacting surface regions to be more accessible in comparison to buried residues in the full-length protein.

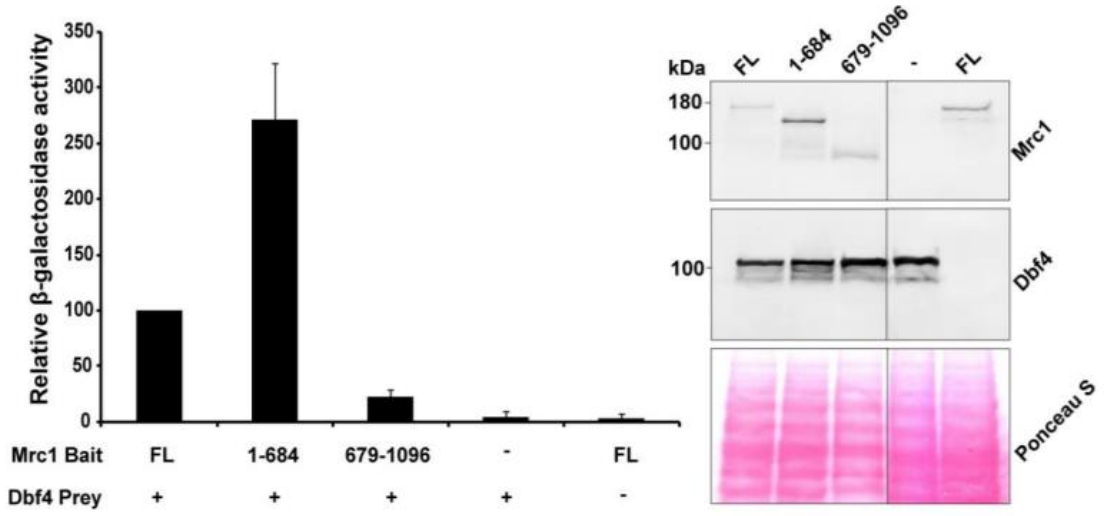

Figure 3.2 Mrc1 interacts with Dbf4 at its N-terminal region. "FL" refers to full length Mrc1 cloned into the bait vector. "1 – 684" and "679 – 1096" denote amino acid residues that make up Mrc1 N and Mrc1 C regions, respectively. pEG202 and pJG4-6 were used as bait and prey vectors, respectively. Yeast two-hybrid results are presented as a percentage of β-galactosidase activity in the Mrc1 FL-Dbf4 trials. Each interaction was evaluated in triplicate independent trials and error bars represent standard deviation. Anti-LexA and anti-HA was used to detect proteins expressed in bait and prey vectors, respectively. Ponceau S staining shows consistent protein loading in each lane. Trials including empty bait or prey vectors were included as controls for β-galactosidase activity and western blotting (Figure reproduced with permission from Larasati, 2020).

3.2 Results

3.2.1 Mrc1 N1.1 Region Mediates Binding to Dbf4

Previous results in the Duncker lab identified a DDK interacting region of Mrc1 that differs in *S. cerevisiae* in comparison to a recent proposed fission yeast model (reviewed in Masai *et al.*, 2017). Specifically, Mrc1 interacts with Dbf4 rather than Cdc7 at its N-terminal region, without the requirement of its C-terminal region. These results imply that Mrc1 does

not maintain intramolecular interactions, as in fission yeast, to recruit DDK. Next, further truncation and Y2H analysis of the Mrc1 N-terminal region was conducted in a similar manner to specify a discrete binding region. The N-terminal region of Mrc1 was separated into N1 and N2 regions, spanning amino acid residues 1 – 373 and 340 – 684, respectively (refer to Figure 2.1 *Mrc1 Regions cloned into pEG202 for Yeast Two-Hybrid*). These truncations were generated to create two similarly sized N-terminal sub-regions, each containing several residues of high sequence conservation in the multiple sequence alignment comparison of budding yeast Mrc1 amongst different fungal species (Lasarati, 2020). Additionally, the region of separation shows low sequence conservation in the same multiple sequence alignment. The Y2H results in figure 3.3 specify the requirement of the Mrc1 N1 region to maintain interactions with Dbf4. Conversely, the Mrc1 N2 region shows minimal binding to Mrc1 and is not required to maintain the interaction observed at the N1 region.

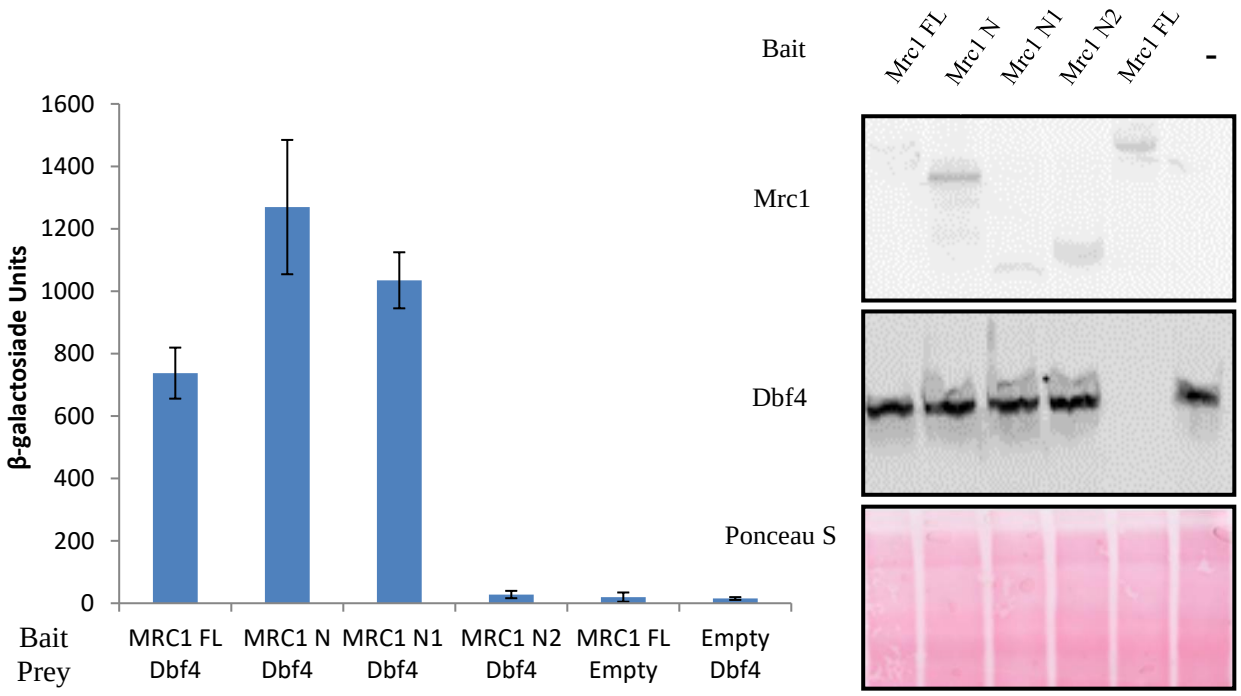

Figure 3.3 Mrc1 interacts with Dbf4 through its N1 region. Each interaction was evaluated in triplicate independent trials and error bars represent standard deviation. pEG202 and pJG4-6 were used as bait and prey vectors, respectively. Anti-LexA and anti-HA was used to detect proteins expressed in bait and prey vectors, respectively. Ponceau S staining shows consistent protein loading in each lane. β-galactosidase activity units = 1000 x A420/ (t x v x A600). A420 is the absorbance of ONP, A600 is the cellular density of the culture, t is the time elapsed, and v is the volume of culture added in ml for 5 x 10^6 cells. Trials including empty bait or prey vectors were included as controls for β-galactosidase activity and western blotting.

A final series of Y2H experiments were conducted with bait constructs Mrc1 N1.1, spanning amino acid residues 1 – 186, and Mrc1 N1.2 spanning amino acid residues 165 – 373. The rationale to determine each region to be amplified was the same as previous constructs, with additional consideration of protein structure. First, the multiple sequence alignment of Mrc1 amongst fungal species was used to identify three well conserved amino

acid residues within the N1 region: 1 – 10, 60 – 69, 298 – 331 (Lasarati, 2020). Truncations were created with the goal of separating the two most N-terminal regions from the larger, more central region in the Mrc1 N1 sequence, creating two peptides of similar sizes. The overlap site at which N1 was split into two new constructs spans amino acid residues 165–186. This is due to the lack of high amino acid conservation as well as a software prediction of an intrinsically disordered region (IDR) at amino acid residues 166 – 200 (MobiDB, 2021) (figure 3.4). MobiDB prediction software uses a consensus method to find IDRs, based upon a UniProt Knowledgebase protein database search. Therefore, the highlighted region in figure 3.4 indicates a predicted IDR which lacks a stable tertiary structure under native conditions (Reviewed in Babu, 2016).

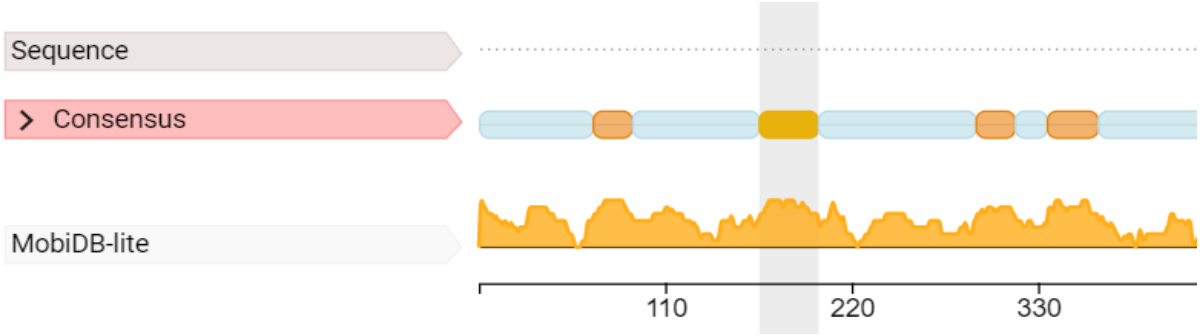

Figure 3.4 Amino acid residues 166 – 200 of Mrc1 is predicted to be a disordered region. MobiDB-lite IDR prediction software was used to analyze the entire Mrc1 sequence. Orange bars in the consensus sequence represent predicted IDRs and blue bars represent predicted protein structures. An MobiDB-lite score is provided in the orange graph, visualizing an estimated score of the predictor software at a specific residue. Amino acid sequence count is represented by the black line.

The results obtained demonstrate that the 186 amino acid N1.1 region interacts with Dbf4, not the N1.2 domain (figure 3.5). Furthermore, an Mrc1 ΔN1.1 mutant sequence (amino acid residues 186 – 1096) was cloned into the pEG202 bait vector and trials were completed to confirm that the interaction is not mediated at any other region of Mrc1. As expected, Mrc1 ΔN1.1 maintained low levels of β-galactosidase activity, similar to the negative controls, confirming that the Mrc1 N1.1 region is both necessary and sufficient in maintaining an interaction with Dbf4 (figure 3.6).

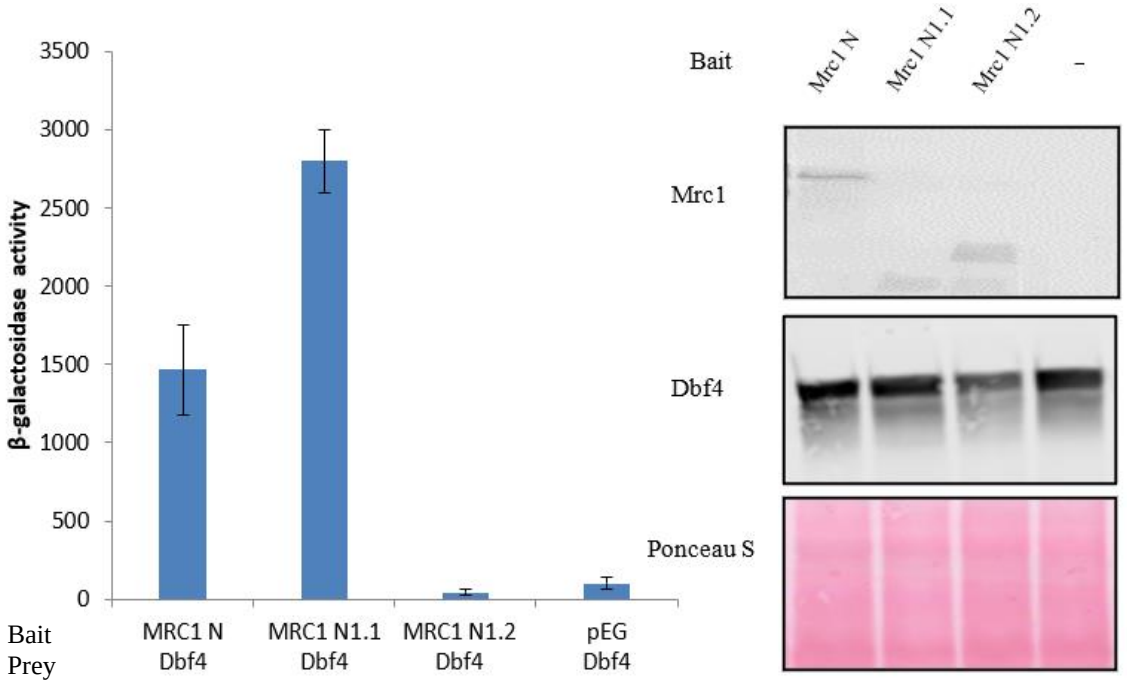

Figure 3.5 Mrc1 interacts with Dbf4 at an N1.1 region. Each interaction was evaluated in triplicate independent trials and error bars represent standard deviation. pEG202 and pJG4-6 were used as bait and prey vectors, respectively. Anti-LexA and anti-HA was used to detect proteins expressed in bait and prey vectors, respectively. Ponceau S staining shows consistent protein loading in each lane. β-galactosidase activity units = 1000 x A420/ (t x v x A600). A420 is the absorbance of ONP, A600 is the cellular density of the culture, t is the time elapsed, and v is the volume of culture added in ml for 5 x 10^6 cells. Trials including empty ait or prey vectors were included as controls for β-galactosidase activity.

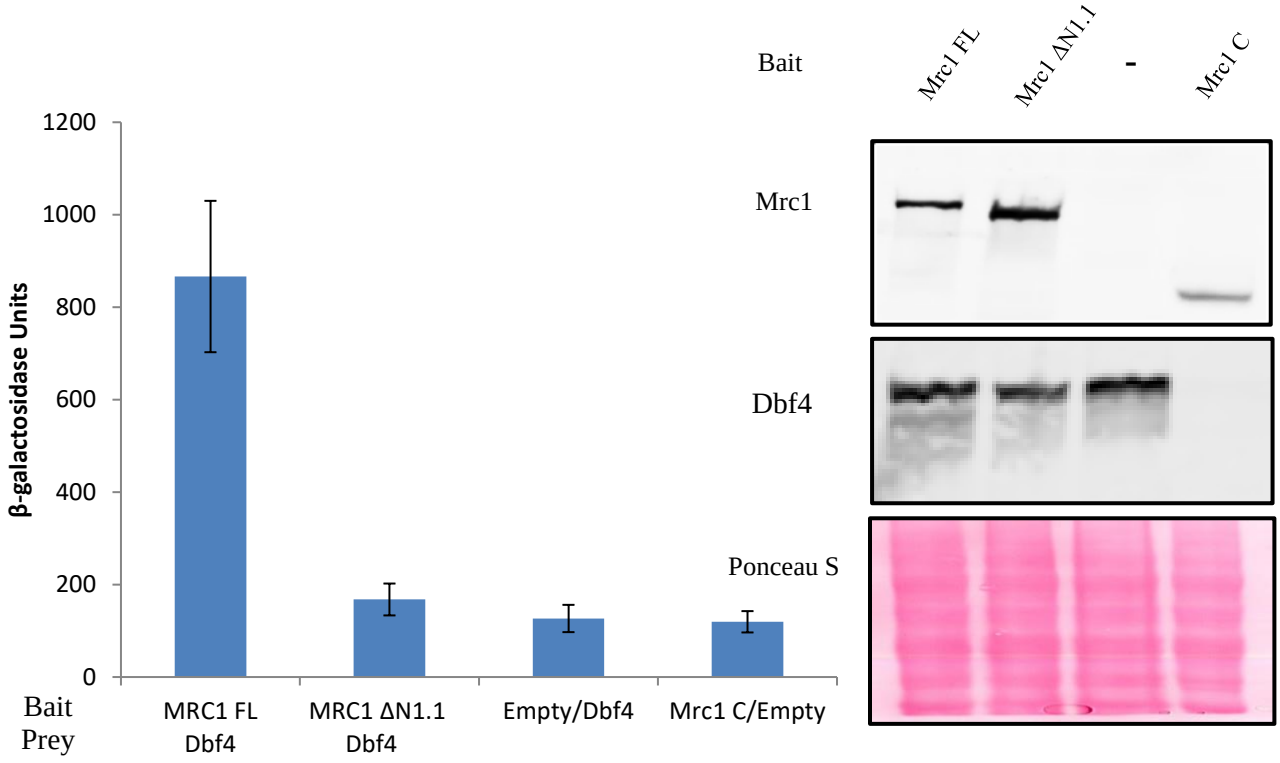

Figure 3.6 Mrc1 ΔN1.1 maintains wildtype growth in the presence of genotoxic stressors. Each strain was serially diluted ten-fold, for a total of 5 times. BioRad ChemiDoc MP systems were used to image plates after 48 hours of growth at 30°C. Spot plates displayed in this figure are representative results that were replicated in three separate trials. Genotoxic agents were added to freshly prepared YPD at the indicated concentrations. Δrad53 was used as a control to confirm the presence of each genotoxic agent.

3.2.2 Mrc1 ΔN1.1 Exhibits a Moderate Growth Defect Under Optimal Growth Conditions

Following the identification of the Mrc1 N1.1 region in maintaining interactions to Dbf4, growth curve trials were conducted to assess phenotypic variations of this mutant in comparison to wildtype and ΔMrc1 knockout controls. Due to the importance of Dbf4 in

origin firing and previous findings of DDK-dependent binding of Mrc1 to early origins, it was hypothesized that an abrogation of the Mrc1-Dbf4 interaction in the Mrc1 ΔN1.1 strain would create a checkpoint-independent growth defect (Osborn & Elledge, 2003). Since Mrc1 is consistently bound to early origins in wildtype strains, the disruption of this interaction in this mutant may impede Mrc1 recruitment to these sites. Although this hypothesis contrasts previous findings of Mrc1 acting as a constraint to origin firing in fission yeast, the binding of Mrc1 to DDK is mediated at a different region of Mrc1 and to a different subunit of DDK in *S. cerevisiae*, indicating a differing mechanism between each yeast (reviewed in Masai et al., 2017).

The growth curve was constructed to evaluate Mrc1 ΔN1.1 growth over a 12-hour time course. Results consistently showed a minor growth defect of Mrc1 ΔN1.1 in comparison to the wildtype culture (figure 3.7). Importantly, the growth defect takes place under optimal growth conditions, supporting the presence of a checkpoint-independent role of Mrc1 in cell cycle progression. The ΔMrc1 strain displayed major growth impediments, likely due to its absence in the other roles such as the FPC and keeping polymerases and helicase components in proximity (Baretić et al., 2020).

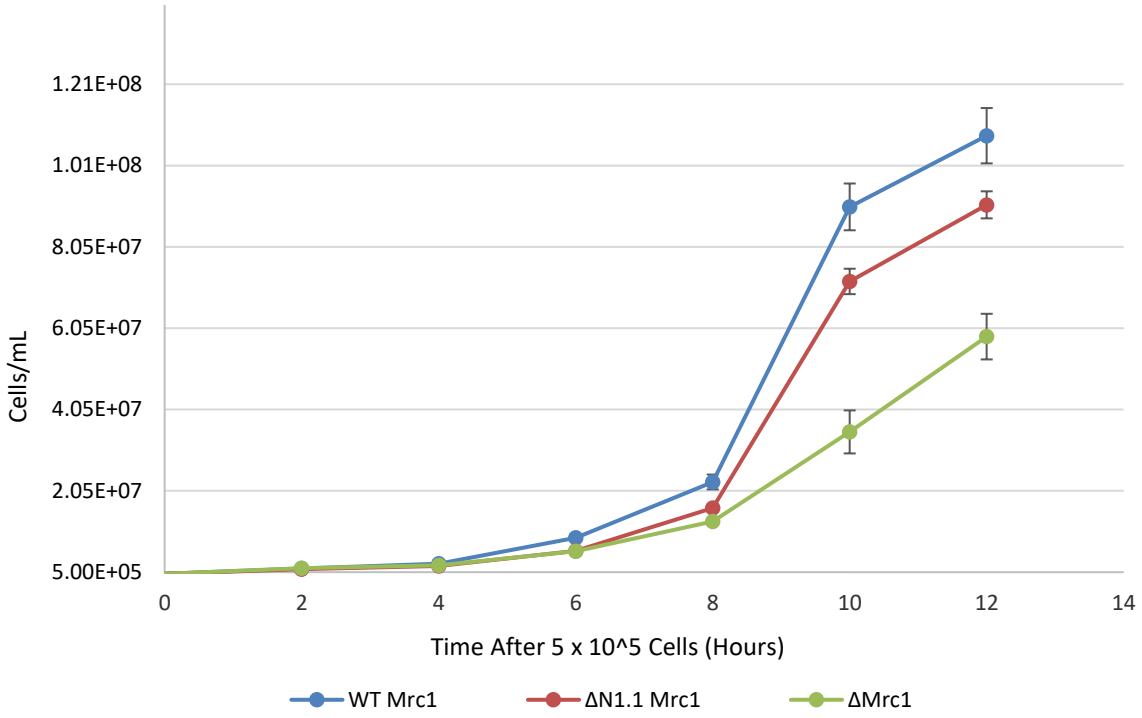

Figure 3.7 Mrc1 ΔN1.1 demonstrates a moderate growth defect under optimal growth conditions. 1 x 10^7 cells/ml working cultures of each strain was diluted to 5 x 10^5 cells/ml in 50 ml of fresh YPD at time point 0 hours. Cultures were grown for a total of 12 hours and cell concentration was measured every 2 hours. Three independent trials were completed, and the standard deviation is represented by error bars.

3.2.3 Mrc1 ΔN1.1 Maintains a Checkpoint Response to Genotoxic Stress

One aspect in confirming the speculative role of Mrc1 ΔN1.1 in checkpoint-independent function is to determine if the growth defect observed in figure 3.7 is due to potential disruption of the checkpoint response. Importantly, the N1.1 region does not include amino acids 266 – 635, which contain three necessary SQ/TQ sites that are critical in maintaining the checkpoint response of Mrc1 to replicative stress (figure 3.8) (Naylor *et al.*,

2009). Similarly, known Mrc1 associations to Tof1 and Ctf4 in the FPC are expected to remain intact within this mutant strain (figure 3.8) (Baretić *et al.*, 2020). Therefore, it is expected that the deletion of the Mrc1 N1.1 region would not disrupt intra-S phase checkpoint signaling. To verify this, spotting growth assays were conducted in the presence of replicative stressors to assess replication checkpoint functionality. The compounds used in this assay include hydroxyurea (HU), bleomycin, phleomycin, and methyl methanesulfonate (MMS). Hydroxyurea is ribonucleotide reductase inhibitor which prevents dNTP production, thus limiting its availability for replication. Bleomycin and phleomycin create double stranded breaks, while MMS modifies guanine and adenine nucleobases to cause base mispairing, DNA lesions, and replication blocks (reviewed in Chen *et al*., 2008). Thus, various compounds introduce replicative stress in different forms, to verify the integrity of different checkpoint response mechanisms.

First, a Mrc1 ΔN1.1 strain was generated and verified using techniques previously described in section 2.1. Spot plate growth amongst all strains was consistent on YPD media without genotoxic agents added (figure 3.9). As expected, ΔMrc1 and Δrad53 strain growth was observed as checkpoint arrest pathways are not induced in this medium. Induced DNA replication stress shows no Δrad53 strain growth at any dilution, verifying the presence of each additive during media preparation. Observed ΔMrc1 strain growth defects were also expected due to its role to facilitate Mec1 phosphorylation of Rad53 under replicative stress. Reduced cell growth at lower dilutions (less than that of the wildtype strain) is still present due to the presence of Rad9. Although Rad9 primarily mediates checkpoints outside of S

phase, this adaptor protein likely increased activity to compensate for the Mrc1 deletion. Finally, the Mrc1 ΔN1.1 strain displays similar growth to the wildtype, indicating an intact role in replication checkpoint. A very miniscule defect of Mrc1 ΔN1.1 growth at the highest dilution series of each plate can be identified as well. However, the consistent presence of this defect in optimal and replicative stress conditions indicates that it is not due to any effect of checkpoint signaling. Instead, a potential source of this growth defect may be a loss of structural integrity in Mrc1 ΔN1.1, which may impact the circular conformation of Mrc1 and strength of DNA binding within its central region (Li & Zhang, 2020).

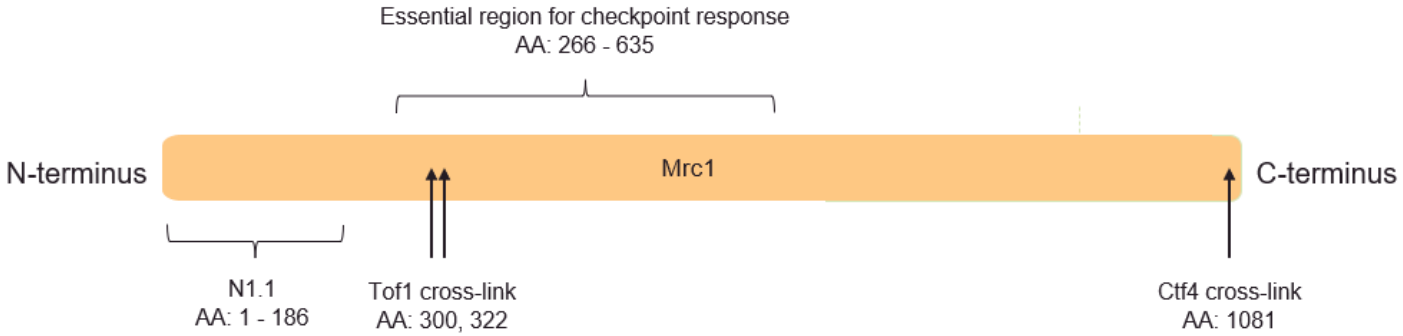

Figure 3.8 Mrc1 ΔN1.1 is Expected to Maintain Checkpoint Function. Mrc1 N1.1 does not reside in regions facilitating known roles of Mrc1. Amino acid region 266 – 635 contains SQ/TQ phosphorylation motifs that are essential for a complete intra-S phase checkpoint response to replicative stress (Naylor et al., 2009). Cross-linking mass spectrometry analysis revealed binding sites of FPC proteins, Tof1 and Ctf4 (Baretić et al., 2020).

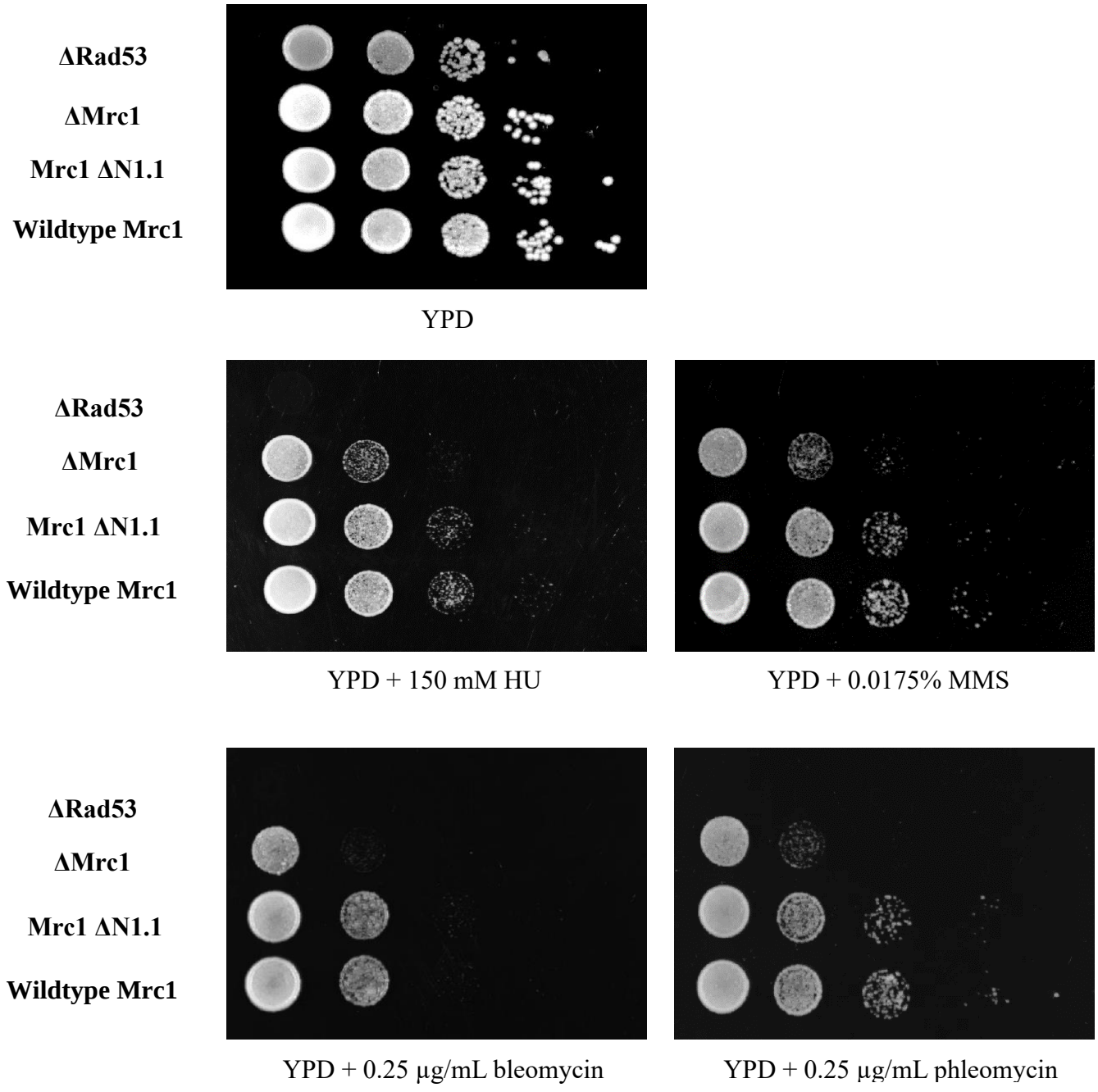

Figure 3.9 Mrc1 ΔN1.1 maintains wildtype growth in the presence of genotoxic stressors. Each strain was serially diluted ten-fold, for a total of 5 times. BioRad ChemiDoc MP systems were used to image plates after 48 hours of growth at 30°C. Spot plates displayed in this figure are representative results that were replicated in three separate trials. Genotoxic agents were added to freshly prepared YPD at the indicated concentrations. Δrad53 was used as a control to confirm the presence of each genotoxic agent.

3.2.4 Identification of Potential DNA Replication Defects in the Mrc1 ΔN1.1 Strain

To further identify the checkpoint-independent growth defect of Mrc1 ΔN1.1, FACS analysis was performed. Here, progression of DNA content through S-phase can be monitored to pinpoint a possible distinct phenotype of the mutant. A ΔMrc1 culture was also included in FACS trials, displaying expected slow S-phase progression in comparision to the wildtype (figure 3.10; panel A and B). When comparing Mrc1 ΔN1.1 with the wildtype, no significant differences in S-phase progression are observed (figure 3.10; panel A and C). This indicates that the disruption of binding Mrc1 to Dbf4 in this mutant did not have an impact on the initiation or progression of DNA replication as previously hypothesized. However, it may be possible that the replication initiation defects in Mrc1 ΔN1.1 are minor and indistinghusiable in the context of FACS cell cycle analysis. Instead, employing methodology that asseses defects in DNA replication over many generations of growth may allow for the accumulation of defects, allowing for discernable differences in comparision to wildtype cells.

To this end, a plasmid stability assay was performed. Briefly, this assay evaluates plasmid loss per generation of growth in cells transformed with a YCplac111 vector, which is maintained at one copy per cell and contains a *leu2* selective marker (Gietz & Sugino, 1988). Transformants were plated on both selective and non-selective media directly after growth in media containing the leucine. Theoretically, strains with a lower rate of plasmid loss per generation indicate an intact DNA replication mechanism, duplicating a copy of the plasmid into daughter cells and allowing for growth in auxotrophic conditions. The results in figure

3.10 represent data from two trials, which must be completed in triplicate to make final conclusions. Based upon the current data, the Mrc1 ΔN1.1 strain had a higher average rate of plasmid loss (2.58%) in comparision to the wildtype strain (1.20%), and similar levels to that of a ΔMrc1 strain (2.74%). This may indicate a deficiency in DNA replication as the low copy number YCpLac111 vector is not being efficiently replicated and therefore not being passed down to daughter cells at the same rate as the wildtype strain.

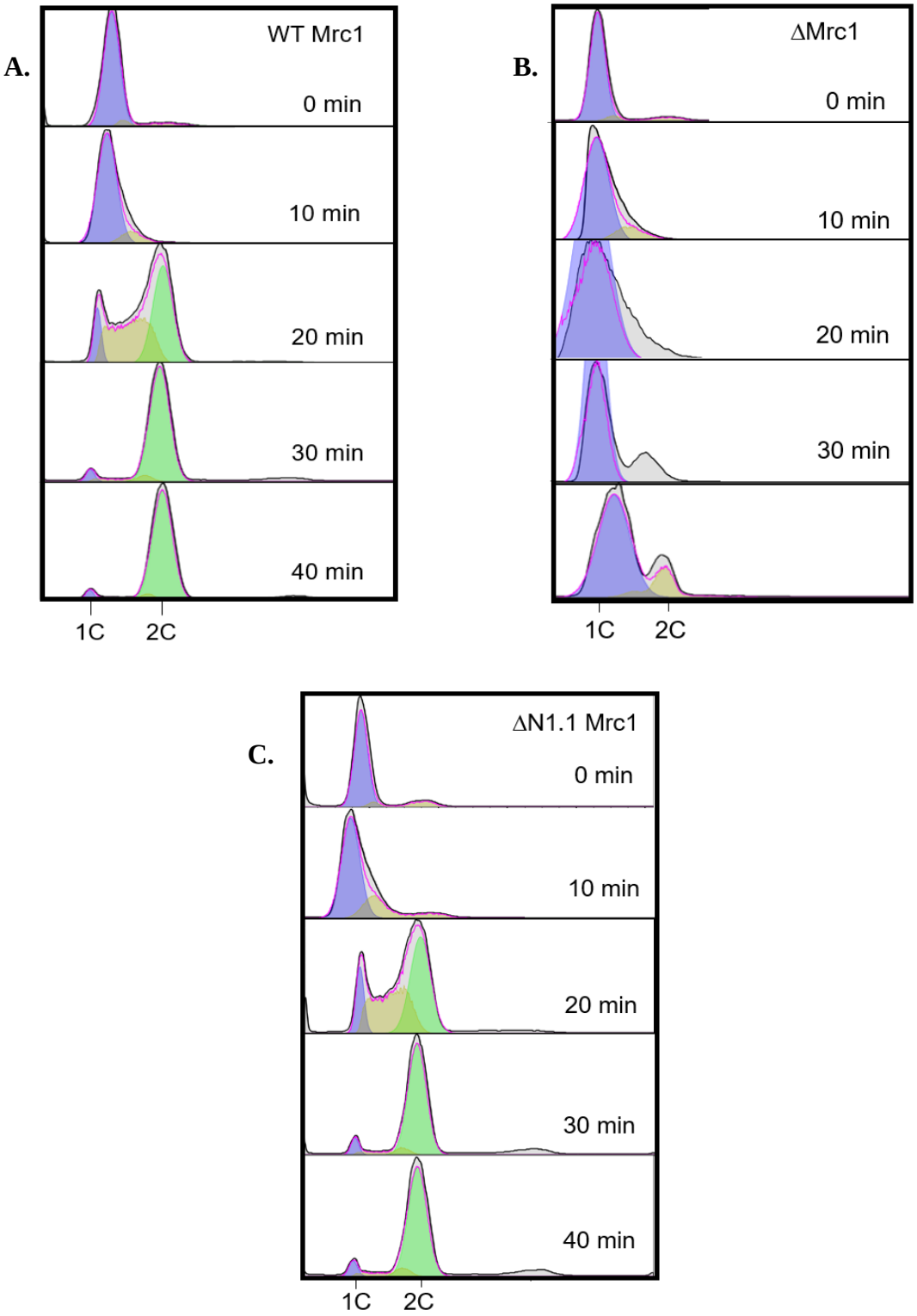
A.
WT Mrc1
0 min
10 min
20 min
30 min
40 min
1C
2C
B.
ΔMrc1
0 min
10 min
20 min
30 min
1C
2C
C.
ΔN1.1 Mrc1
0 min
10 min
20 min
30 min
40 min
1C
2C

Figure 3.10 Mrc1 ΔN1.1 maintains normal S-phase progression in FACS analysis. Asyncronous cultures were arrested in G1 with the addition of 40 µg/ml α-factor and incubation for 2.5 hours at 30°C. Cultures were released from arrest by the addition of 50 µg/ml Pronase E (Sigma). Coloured areas of FACS results indicate distinct phases: purple represents G1 phase, yellow represents S phase, green represents G2 phase. The absence of genome duplication is denoted as 1C and 2C represents complete replication of genomic content. FACS analysis was completed by Justin Law and Bradley D'souza. Visualization of FACS data was completed by Justin Law using FlowJo™ Software (BD Life Sciences).

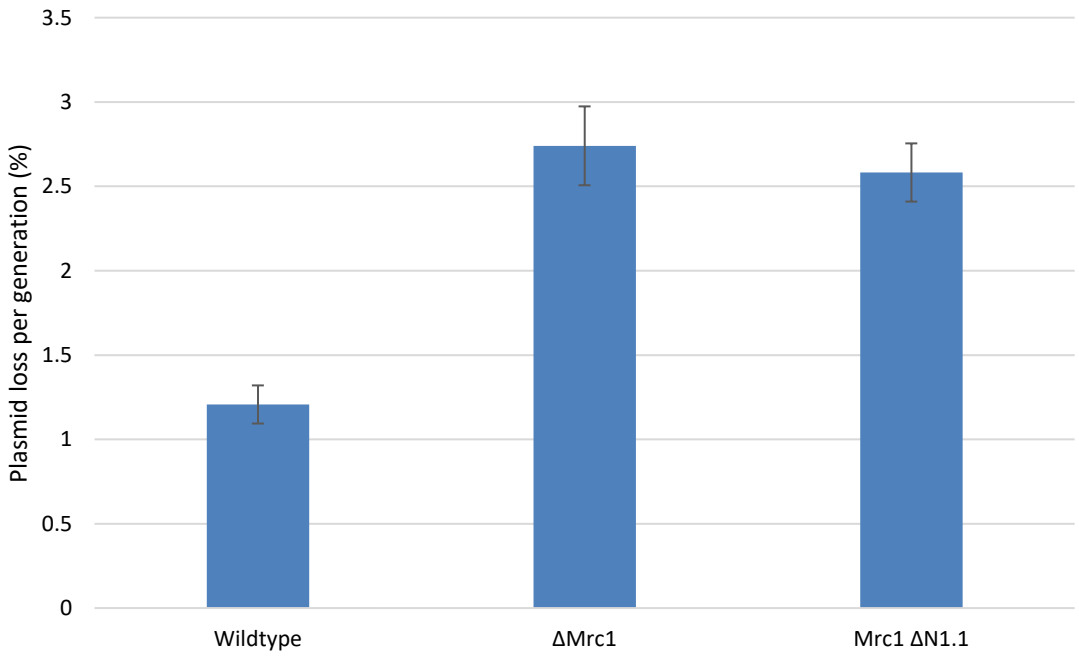

Figure 3.11 Mrc1 ΔN1.1 may have a higher rate of plasmid loss per generation in comparision to wildtype cells. YCplac111 vector was transformed into each strain and plated on 10 YPD and 10 SC-leu agar medium to asess plasmid stability and replication (60 plates in total for 3 strains). All plates were incubated at 30°C for 48 hours and colonies were counted using a Quebec Colony Counter. Plasmid loss per generation = (1- (colony number on SC-leu/colony number on YPD))/number of cell divisions. Results in this graph represent a single trial. Plasmid stability assay trials were completed by Bradley D'souza and Mike Meleka.

Statistical analysis was completed for the plasmid loss assay, beginning by quantifying the percentage difference of Mrc1 ΔN1.1 plasmid loss per generation in comparision to ΔMrc1 and wiltype strains. On average, Mrc1 ΔN1.1 exhibited 1.417% more plasmid loss per generation than the wildtype and 0.201% less plasmid loss per generation than ΔMrc1. Therefore, it is evident that the difference in Mrc1 ΔN1.1 plasmid loss per generation is substantially higher when compared to the wildtype and marginal in relation to ΔMrc1. To validate these results, the primary objective was to determine if the difference between Mrc1 ΔN1.1 and the wildtype strain is significant. A secondary objective was to determine if the difference between Mrc1 ΔN1.1 and ΔMrc1 strains is insigficant. First, colony counts of each strain on SC-leu media was standardized to account for optimal growth on YPD plates. To this end, YPD colony count data was treated as the population when determining standard score values, which is expressed by the following equation:

$$z = \frac{x - \mu}{\sigma}$$

x = SC-leu colony count for a single plate

μ = mean of YPD colony counts (population mean)

σ = standard deviation of YPD colony counts

A scatter plot highlighting the SC-leu standard score values for each strain is displayed in Appendix B.

These standardized values were used to conduct hypothesis testing. Student's t-test was used to generate p-values for each strain because the total number of SC-leu plates was relatively low (20 per strain). The confidence level used for hypothesis testing is 99%. The null hypothesis (H_0) and alternate hypothesis (H_a) are as follows:

H_0 = The mean of Mrc1 ΔN1.1 standard score values (sample mean) is not significantly different in comparision to the population mean.

H_a = The mean of Mrc1 ΔN1.1 standard score values (sample mean) is significantly different in comparision to the population mean.

For the primary objective, the wildtype standard score values were used as the population, whereas ΔMrc1 standard score values were used as the population for the secondary objective.

Table 3.1 Plasmid Loss Assay p-values for Strain Comparisons

	Mrc1 ΔN1.1 (DY-391) vs. Wildtype (DY-30)	Mrc1 ΔN1.1 (DY-391) vs. ΔMrc1 (DY-298)
Population Mean	-1.412	-4.343
Sample Mean	-4.658	-4.658
Sample Standard Deviation	0.616	0.616
Degrees of freedom	19	19
t-value	-23.557	-2.288
p-value	< 0.00001	0.034

The null hypothesis is rejected for p-values less than 0.01 and not rejected for p-values greater than 0.01. As displayed in table 3.1, the p-value for the comparison between Mrc1 ΔN1.1 and the wildtype is less than 0.01, indicating that the large difference in plasmid loss per generation between these strains is statistically significant. In contrast, the p-value when comparing Mrc1 ΔN1.1 and ΔMrc1 is 0.034, indicating that the difference in plasmid loss per generation between these strains is statistically insignificant. Overall, these results support the findings that the plasmid loss per generation in Mrc1 ΔN1.1 is likely due to defects in DNA replication stability caused by the deletion of the N1.1 region, rather than exogenous factors.

Chapter 4: General Conclusions and Future Directions

4.1 Mrc1 N1.1 is Necessary and Sufficient for Binding to Dbf4. Mrc1 ΔN1.1 Exhibits a Moderate Growth Defect While Maintaining Checkpoint Function

Protein-protein interactions between Mrc1 and DDK have been identified and characterized in the past. These have been demonstrated in various eukaryotes, such as human Cdc7 phosphorylating and interacting with Claspin in HeLa cells, and the more recent model of Mrc1 binding to Hsk1 at the site of intramolecular interactions in fission yeast (Kim *et al.*, 2008; reviewed in Masai *et al.*, 2017). However, initial confirmation of the same interaction in budding yeast has revealed binding of Mrc1 to Dbf4, rather than Cdc7 (Larasati, 2020). Importantly, this interaction that takes place at a Mrc1 N-terminal region has not been identified in other eukaryotes and implicates a novel mechanism. Further characterization of this interaction is of great interest due to increasing evidence of a checkpoint-independent function of Mrc1 that affects origin timing in eukaryotes (reviewed in section 1.3.2). Since DDK is an essential component of the replication initiation process, a better understanding of its mechanism with Mrc1 may be relevant for higher eukaryotes and eventual clinical applications.

First, several series of Y2H assays with N-terminal Mrc1 truncations revealed that an N1.1 region, amino acid residues 1 – 186, is both necessary and sufficient for maintaining interactions with Dbf4. The absence of protein-protein interactions at Mrc1s C-terminus, unlike fission yeast and human orthologs, also provides further evidence of a novel mechanism in budding yeast that may not involve an intramolecular interaction binding site. This is supplemented by the lack of sequence conservation of the intramolecular interaction

sites at N- and C-terminal regions of budding yeast when compared to HBS and NTHBS regions in *S. pombe* (Masai *et al.*, 2011).

Growth curve comparisons revealed Mrc1 ΔN1.1 had a growth defect, exhibiting a slightly slower rate of growth than the wildtype strain and a significantly higher growth rate than the ΔMrc1 strain. This result was significant as it demonstrated a phenotypic variance from the wildtype strain specifically due to the deletion of the N1.1 region. Since the growth curve was conducted in the absence of any DNA replication stressors, this implicates a defect during normal cell cycle progression. Furthermore, the slow growth rate is specifically due to the disruption of an Mrc1-Dbf4 interaction, supporting a potential role of Mrc1 in normal checkpoint-independent cell cycle progression.

The next goal was to verify checkpoint response functionality of Mrc1 ΔN1.1. The checkpoint role of Mrc1 is well characterized and so it was important to maintain function when identifying phenotypic changes in a newly generated mutant. A Mrc1 ΔN1.1 mutant was hypothesized to maintain checkpoint function due to previous findings of a larger N-terminal truncation, Mrc1-N4, which conferred HU resistance to a similar extent observed for wildtype cells (Naylor *et al*., 2009). Furthermore, Mrc1 regions which interact with FPC components Ctf4 and Tof1 remain intact in a ΔN1.1 mutant (Baretic *et al*., 2020). A Mrc1 ΔN1.1 strain (DY-391) was generated and subjected to a spot plate assay in the presence of various genotoxic stressors. Sensitivity of Mrc1 ΔN1.1 in all plates was comparable to the wildtype strain, indicating a functional checkpoint response. The type of replicative stress did not impact growth, whether it was direct DNA double-stranded breaks (phleomycin and

bleomycin) or depletion of dNTP pools, indicating functionality of differing Rad53 downstream pathways. This reproducible result confirmed the hypothesis that Mrc1 ΔN1.1 exhibits a modest growth defect, speculated to be due to an affected role in DNA replication initiation, while maintaining a functional checkpoint response.

4.2 FACS Analysis Reveals Unchanged S-Phase Progression in Mrc1 ΔN1.1, But A Compounded Replication Defect is Observed in Plasmid Stability Assay

FACS analysis was conducted to specify if the growth defect examined was specifically due to impaired DNA replication, which would be exhibited by slow S-phase progression. Since DDK is a necessary complex to fire origins, disruption of its interaction with Mrc1 was hypothesized to create a slower growth rate specifically during DNA replication initiation. This would be consistent with the presence of Mrc1 at several early origins and an increase in DNA replication rates to a maximum in the presence of wildtype Mrc1 within an *in vitro* replication assay (Yeeles et al., 2017). Conversely, recent findings in fission yeast demonstrated earlier and more efficient firing of several early origins in Δmrc1 in the absence of genotoxic stress. FACS analysis revealed S-phase progression of Mrc1 ΔN1.1 was equivalent to that of the isogenic wildtype strain. This implies that the ΔN1.1 growth defect exhibited in the growth curve trials was not due to deficiencies in DNA replication. However, preliminary plasmid stability assay results from two trials revealed a higher rate of plasmid loss per generation in ΔN1.1 cells (similar to ΔMrc1) in comparison to wildtype cells. Plasmid duplication into daughter cells requires intact DNA replication mechanisms, indicating DNA replication instability in ΔN1.1 background. However, it is

well esthablished that natural plasmid loss rates of yeast centromere vectors is 1 – 3% per generation, and so the plasmid stability assay results do not indicate a large DNA replication defect (Dani *et al*., 1983). The consistently higher plasmid loss rates amongst several trials still indicates a minor DNA replication defect that has significant impliciations after a compounded affect over multiple generations of growth.

The findings within this thesis are another example of how budding yeast can be used to identify novel interactions that are relevant to DNA replication. An overexpression of DDK is correlated with several cancers and so the interaction with Mrc1 is of great intrest as a possiblility of regulating this essential kinase complex (Sasi et al., 2017). The findings outlined here indicate a growth defect due to DNA replication instability when the Mrc1-Dbf4 interaction is abrograted. The interplay between these two proteins would have to be explored in much greater detail to develop a mechanistic understanding, but these findings still provide further evidence for the speculated Mrc1 checkpoint-independent role. As further details of Mrc1s role in DNA replication are revealed, targeting of this protein within higher eukaryotes may be a viable strategy in developing cancer treatments.

4.3 Future Directions

An immediate goal following the conclusions made in this thesis is to conduct ChIP trials including Mrc1-Myc and Mrc1 ΔN1.1-Myc strains to examine loading onto candidate early and late firing origins. Temporal association patterns of this mutant binding to these DNA regions can reveal details regarding a potential mode of replication initiation

regulation. For instance, delayed binding kinetics of Mrc1 ΔN1.1 onto early origins would provide insight regarding the growth defects that were observed under normal growth conditions. In this case, Dbf4 recruitment can be subsequently assessed to verify if the ΔN1.1 mutation is delaying recruitment of the essential origin firing kinase complex.

First, the ChIP protocol was optimized based upon previous iterations within the Duncker lab (DaSilva and Duncker, 2007) (Ramer *et al*., 2013). All changes are indicated in section 2.8, with most notable changes being made to the ChIP PCR conditions. Optimization trials were conducted using an asynchronous Orc2-Myc (DY-81) culture, examining ARS305 and ARS1 binding, because Orc2 is stably origin bound throughout the cell cycle (Bell and Dutta, 2002). Initial results indicate successful ChIP pull down of Orc2-bound DNA at both origin sites (Appendix A Figure 1, panels A and B). For the Input (IN) samples within lane 2 of both agarose gels, amplification of both origin flanking and origin specific regions is present (upper band = 9kb upstream non-origin sequence, middle band = ARS1/ARS305 specific sequence, lower band = 9kb downstream non-origin sequence). This is expected because the input fraction is obtained before Dynabead pull-down, containing all cellular DNA. As a result, template DNA is available for all three regions of interest. In contrast, amplification of only the ARS305 or ARS1 specific sequences is primarily observed for the immunoprecipitated (IP) sample within lane 3 of both agarose gels. Once again, this is expected because the IP fraction should only contain DNA that is specifically bound to Orc2-Myc after Dynabead pulldown and purification. Optimized conditions based upon Orc2-Myc trials are now being applied to asynchronous ChIP trials with Mrc1-Myc (DY-394) and Mrc1

ΔN1.1-Myc (DY-395) strains. If asynchronous ChIP amongst these strains is successful, synchronous release from G1 arrest would be the following step to assess loading onto early origins over regular time intervals. ChIP PCR can also be conducted at candidate late origins, such as ARS603, allowing for comparisons of Mrc1 loading efficiency between early and late origins. Within these trials Dbf4 loading to the same origins could be identified as well, allowing for further details to be revealed regarding recruitment timing of Mrc1 and Dbf4. For instance, delayed Dbf4 recruitment to origins in a Mrc1 ΔN1.1 background would cause delayed origin firing, which may be the basis for the moderate growth curve defect observed in figure 3.7.

Y2H Mrc1 N1.1-Dbf4 protein-protein interactions will also be confirmed using coimmunoprecipitation analysis. The fission yeast model developed by Masai and colleagues in 2017 is largely based upon coimmunoprecipitation results and completing similar experiments will verify current findings in the Duncker lab and allow for direct comparisons to be made. Another confirmatory measure to complete is the assessment of Rad53 phosphorylation in the Mrc1 ΔN1.1 strain, to verify intact checkpoint functionality. Effective Rad53 phosphorylation could simply be detected by slower migration of the protein in comparison to wildtype on SDS-PAGE and subsequent western blot analysis. DDK dependent phosphorylation of Mcm2-7 subunits is also of great interest to determine the effect of a Mrc1 ΔN1.1 on replication initiation. Throughout all future ChIP, coimmunoprecipitation, and phosphorylation state studies, an important aspect to consider is the structural integrity of Mrc1 ΔN1.1. Electron microscopy reconstitution techniques that

have recently revealed the circular wildtype Mrc1 structure in budding yeast can be employed to confirm the stability of this new mutant (Li & Zhang, 2020). If there is loss in the circular structure or DNA density to the hole in the middle, this may indicate structural instability and any findings within Mrc1 ΔN1.1 would then need to be reassessed.

Regarding the N1.1 region, further truncations can be made to further specify a discrete binding region that maintains an interaction with Dbf4. Subsequent alanine scanning site-directed mutagenesis can be performed to determine specific amino acid residue requirements in this region. Finally, the primary focus of this thesis is on the region of Mrc1 that facilitates protein-protein interactions with Dbf4. However, determination of the binding domain on the sequence of Dbf4 is important in characterizing the interaction in the future. As mentioned previously, Dbf4 has three conserved motifs: N (N-terminal), M (medial), and C (C-terminus), with each name denoting relative amino acid positions. Previous preliminary data has identified the N and C motifs to be necessary in maintaining an interaction with Mrc1 (Larasati, 2020). In contrast, a complete deletion of the M region did not have any significant effect on the strength of Dbf4-Mrc1 interactions. The C motif is known to contain a zinc finger that is required for Cdc7 activation and so this region may be of great interest with respect to Mrc1 binding (Jones et al., 2010). Additionally, the requirement of both terminal ends may indicate a potential intramolecular Dbf4 interaction, at which binding to Mrc1 occurs.

References

Abd Wahab, S., & Remus, D. (2020). Antagonistic control of DDK binding to licensed replication origins by Mcm2 and Rad53. *ELife*, *9*, e58571.

Alver, R. C., Chadha, G. S., & Blow, J. J. (2014). The contribution of dormant origins to genome stability: From cell biology to human genetics. *DNA Repair*, *19*, 182–189.

Aparicio, O. M., Weinstein, D. M., & Bell, S. P. (1997). Components and Dynamics of DNA Replication Complexes in S. cerevisiae: Redistribution of MCM Proteins and Cdc45p during S Phase. *Cell*, *91*, 59–69.

Babu, M. M. (2016). The contribution of intrinsically disordered regions to protein function, cellular complexity, and human disease. *Biochemical Society Transactions*, *44*, 1185–1200.

Bacal, J., Moriel-Carretero, M., Pardo, B., Barthe, A., Sharma, S., Chabes, A., Pasero, P. (2018). Mrc1 and Rad9 cooperate to regulate initiation and elongation of DNA replication in response to DNA damage. *The EMBO Journal*, *37*, e99319.

Baretić, D., Jenkyn-Bedford, M., Aria, V., Cannone, G., Skehel, M., & Yeeles, J. T. P. (2020). Cryo-EM Structure of the Fork Protection Complex Bound to CMG at a Replication Fork. *Molecular Cell*, *78*, 926–940.

Bell, S. P., & Dutta, A. (2002). DNA replication in eukaryotic cells. *Annual Review of Biochemistry*, *71*, 333–374.

Brewer, B. J., & Fangman, W. L. (1987). The localization of replication origins on ARS plasmids in S. cerevisiae. *Cell*, *51*, 463–471.

Cartagena-Lirola, H., Guerini, I., Manfrini, N., Lucchini, G., & Longhese, M. P. (2008). Role of the Saccharomyces cerevisiae Rad53 Checkpoint Kinase in Signaling Double-Strand Breaks during the Meiotic Cell Cycle. *Molecular and Cellular Biology*, *28*, 4480–4493.

Dani, G. M., & Zakian, V. A. (1983). Mitotic and meiotic stability of linear plasmids in yeast. *Proceedings of the National Academy of Sciences of the United States of America*, *80*, 3406–3410.

Das, S. P., Borrman, T., Liu, V. W. T., Yang, S. C.-H., Bechhoefer, J., & Rhind, N. (2015). Replication timing is regulated by the number of MCMs loaded at origins. *Genome Research*, *25*, 1886–1892.

Da-Silva, L. F., & Duncker, B. P. (2007). ORC function in late G1: Maintaining the license for DNA replication. *Cell Cycle (Georgetown, Tex.)*, *6*, 128–130.

Davis, L., & Maizels, N. (2011). G4 DNA: At risk in the genome. *The EMBO Journal*, *30*, 3878–3879.

Dickinson, J. R., & Schweizer, M. (Eds.). (2004). *Metabolism and Molecular Physiology of Saccharomyces Cerevisiae* (2nd ed.). Boca Raton: CRC Press.

Duina, A. A., Miller, M. E., & Keeney, J. B. (2014). Budding Yeast for Budding Geneticists: A Primer on the Saccharomyces cerevisiae Model System. *Genetics*, *197*, 33–48.

Duncker, B. P., Shimada, K., Tsai-Pflugfelder, M., Pasero, P., & Gasser, S. M. (2002). An N-terminal domain of Dbf4p mediates interaction with both origin recognition complex (ORC) and Rad53p and can deregulate late origin firing. *Proceedings of the National Academy of Sciences of the United States of America*, *99*, 16087–16092.

Engel, S. R., & Cherry, J. M. (2013). The new modern era of yeast genomics: Community sequencing and the resulting annotation of multiple Saccharomyces cerevisiae strains at the Saccharomyces Genome Database. *Database: The Journal of Biological Databases and Curation*, *2013*, bat012.

Ferreira, M. F., Santocanale, C., Drury, L. S., & Diffley, J. F. (2000). Dbf4p, an essential S phase-promoting factor, is targeted for degradation by the anaphase-promoting complex. *Molecular and Cellular Biology*, *20*, 242–248.

Gietz, R. D., & Sugino, A. (1988). New yeast-Escherichia coli shuttle vectors constructed with in vitro mutagenized yeast genes lacking six-base pair restriction sites. *Gene*, *74*, 527–534.

Goffeau, A., Barrell, B. G., Bussey, H., Davis, R. W., Dujon, B., Feldmann, H., … Oliver, S. G. (1996). Life with 6000 Genes. *Science*, *274*, 546–567.

Gold, D. A., & Dunphy, W. G. (2010). Drf1-dependent Kinase Interacts with Claspin through a Conserved Protein Motif. *The Journal of Biological Chemistry*, *285*, 12638–12646.

Haber, J. E. (2012). Mating-Type Genes and MAT Switching in Saccharomyces cerevisiae. *Genetics*, *191*, 33–64.

Hayano, M., Kanoh, Y., Matsumoto, S., & Masai, H. (2011). Mrc1 marks early-firing origins and coordinates timing and efficiency of initiation in fission yeast. *Molecular and Cellular Biology*, *31*, 2380–2391.

Heller, R. C., Kang, S., Lam, W. M., Chen, S., Chan, C. S., & Bell, S. P. (2011). Eukaryotic origin-dependent DNA replication in vitro reveals sequential action of DDK and S-CDK kinases. *Cell*, *146*, 80–91.

Herskowitz, I. (1988). Life cycle of the budding yeast Saccharomyces cerevisiae. *Microbiological Reviews*, *52*, 536–553.

Hoggard, T., Müller, C. A., Nieduszynski, C. A., Weinreich, M., & Fox, C. A. (2020). Sir2 mitigates an intrinsic imbalance in origin licensing efficiency between early- and late-replicating euchromatin. *Proceedings of the National Academy of Sciences of the United States of America*, *117*, 14314–14321.

Hughes, S., Elustondo, F., Di Fonzo, A., Leroux, F. G., Wong, A. C., Snijders, A. P., Cherepanov, P. (2012). Crystal structure of human CDC7 kinase in complex with its activator DBF4. *Nature Structural & Molecular Biology*, *19*, 1101–1107.

Jones, D. R., Prasad, A. A., Chan, P. K., & Duncker, B. P. (2010). The Dbf4 motif C zinc finger promotes DNA replication and mediates resistance to genotoxic stress. *Cell Cycle (Georgetown, Tex.)*, *9*, 2018–2026.

Kapoor, P., Shire, K., & Frappier, L. (2001). Reconstitution of Epstein–Barr virus-based plasmid partitioning in budding yeast. *The EMBO Journal*, *20*, 222–230.

Kawasaki, Y., Kim, H.-D., Kojima, A., Seki, T., & Sugino, A. (2006). Reconstitution of Saccharomyces cerevisiae prereplicative complex assembly in vitro. *Genes to Cells*, *11*, 745–756.

Kegel, A., Betts-Lindroos, H., Kanno, T., Jeppsson, K., Ström, L., Katou, Y., … Sjögren, C. (2011). Chromosome length influences replication-induced topological stress. *Nature*, *471*, 392–396.

Kim, J. M., Kakusho, N., Yamada, M., Kanoh, Y., Takemoto, N., & Masai, H. (2008). Cdc7 kinase mediates Claspin phosphorylation in DNA replication checkpoint. *Oncogene*, *27*, 3475–3482.

Köhler, C., Koalick, D., Fabricius, A., Parplys, A. C., Borgmann, K., Pospiech, H., & Grosse, F. (2016). Cdc45 is limiting for replication initiation in humans. *Cell Cycle*, *15*, 974–985.

Koren, A., Soifer, I., & Barkai, N. (2010). MRC1-dependent scaling of the budding yeast DNA replication timing program. *Genome Research*, *20*, 781–790.

Lacroute, F. (1968). Regulation of Pyrimidine Biosynthesis in Saccharomyces cerevisiae. *Journal of Bacteriology*, *95*, 824–832.

Larasati (2020). The characterization of Dbf4 interactions and roles in genome replication and stability in Saccharomyces cerevisiae. UWSpace.

Larasati, & Duncker, B. P. (2016). Mechanisms Governing DDK Regulation of the Initiation of DNA Replication. *Genes*, *8*, E3.

Li, L., & Zhang, Z. (2020). Recombinant expression and characterization of yeast Mrc1, a DNA replication checkpoint mediator. *Preparative Biochemistry & Biotechnology*, *50*, 198–203.

Longtine, M. S., Mckenzie III, A., Demarini, D. J., Shah, N. G., Wach, A., Brachat, A., … Pringle, J. R. (1998). Additional modules for versatile and economical PCR-based gene deletion and modification in Saccharomyces cerevisiae. *Yeast*, *14*, 953–961.

Maicas, S. (2020). The Role of Yeasts in Fermentation Processes. *Microorganisms*, *8*, 1142.

Masai, H., Yang, C.-C., & Matsumoto, S. (2017). Mrc1/Claspin: A new role for regulation of origin firing. *Current Genetics*, *63*, 813–818.

Matthews, L. A., Jones, D. R., Prasad, A. A., Duncker, B. P., & Guarné, A. (2012). Saccharomyces cerevisiae Dbf4 Has Unique Fold Necessary for Interaction with Rad53 Kinase. *The Journal of Biological Chemistry*, *287*, 2378–2387.

Montagnoli, A., Tenca, P., Sola, F., Carpani, D., Brotherton, D., Albanese, C., & Santocanale, C. (2004). Cdc7 inhibition reveals a p53-dependent replication checkpoint that is defective in cancer cells. *Cancer Research*, *64*, 7110–7116.

Muramatsu, S., Hirai, K., Tak, Y.-S., Kamimura, Y., & Araki, H. (2010). CDK-dependent complex formation between replication proteins Dpb11, Sld2, Pol (epsilon), and GINS in budding yeast. *Genes & Development*, *24*, 602–612.

Naylor, M. L., Li, J., Osborn, A. J., & Elledge, S. J. (2009). Mrc1 phosphorylation in response to DNA replication stress is required for Mec1 accumulation at the stalled fork. *Proceedings of the National Academy of Sciences of the United States of America*, *106*, 12765–12770.

Neiman, A. M. (2011). Sporulation in the Budding Yeast Saccharomyces cerevisiae. *Genetics*, *189*, 737–765.

Oehlen, L. J., & Cross, F. R. (1994). G1 cyclins CLN1 and CLN2 repress the mating factor response pathway at Start in the yeast cell cycle. Genes & Development, 8, 1058–1070.

Osborn, A. J., & Elledge, S. J. (2003). Mrc1 is a replication fork component whose phosphorylation in response to DNA replication stress activates Rad53. *Genes & Development*, *17*, 1755–1767.

Parenteau, J., Maignon, L., Berthoumieux, M., Catala, M., Gagnon, V., & Abou Elela, S. (2019). Introns are mediators of cell response to starvation. *Nature*, *565*, 612–617.

Piovesan, D., Necci, M., Escobedo, N., Monzon, A. M., Hatos, A., Mičetić, I., … Tosatto, S. C. E. (2021). MobiDB: Intrinsically disordered proteins in 2021. *Nucleic Acids Research*, *49*, D361–D367.

Prorok, P., Artufel, M., Aze, A., Coulombe, P., Peiffer, I., Lacroix, L., … Méchali, M. (2019). Involvement of G-quadruplex regions in mammalian replication origin activity. *Nature Communications*, *10*, 3274.

Radecka, D., Mukherjee, V., Mateo, R. Q., Stojiljkovic, M., Foulquié-Moreno, M. R., & Thevelein, J. M. (2015). Looking beyond Saccharomyces: The potential of non-conventional yeast species for desirable traits in bioethanol fermentation. *FEMS Yeast Research*, *15*.

Raghuraman, M. K., Winzeler, E. A., Collingwood, D., Hunt, S., Wodicka, L., Conway, A., Fangman, W. L. (2001). Replication dynamics of the yeast genome. *Science (New York, N.Y.)*, *294*, 115–121.

Ramer, M. D., Suman, E. S., Richter, H., Stanger, K., Spranger, M., Bieberstein, N., & Duncker, B. P. (2013). Dbf4 and Cdc7 Proteins Promote DNA Replication through Interactions with Distinct Mcm2–7 Protein Subunits. *The Journal of Biological Chemistry*, *288*, 14926–14935.

Riera, A., Barbon, M., Noguchi, Y., Reuter, L. M., Schneider, S., & Speck, C. (2017). From structure to mechanism—Understanding initiation of DNA replication. *Genes & Development*, *31*, 1073–1088.

Rudner, A. D., & Murray, A. W. (2000). Phosphorylation by Cdc28 activates the Cdc20-dependent activity of the anaphase-promoting complex. *The Journal of Cell Biology*, *149*, 1377–1390.

Sar, F., Lindsey-Boltz, L. A., Subramanian, D., Croteau, D. L., Hutsell, S. Q., Griffith, J. D., & Sancar, A. (2004). Human claspin is a ring-shaped DNA-binding protein with high affinity to branched DNA structures. *The Journal of Biological Chemistry*, *279*, 39289–39295.

Sasi, N. K., Bhutkar, A., Lanning, N. J., MacKeigan, J. P., & Weinreich, M. (2017). DDK Promotes Tumor Chemoresistance and Survival via Multiple Pathways. *Neoplasia (New York, N.Y.)*, *19*, 439–450.

Schreiber, K., Csaba, G., Haslbeck, M., & Zimmer, R. (2015). Alternative Splicing in Next Generation Sequencing Data of Saccharomyces cerevisiae. *PLoS ONE*, *10*, e0140487.

Segal, M., & Bloom, K. (2001). Control of spindle polarity and orientation in Saccharomyces cerevisiae. *Trends in Cell Biology*, *11*, 160–166.

SGD project. “Saccharomycese genome database” http://www.yeastgenome.org. (November 2nd, 2021)

Sheu, Y.-J., Kinney, J. B., Lengronne, A., Pasero, P., & Stillman, B. (2014). Domain within the helicase subunit Mcm4 integrates multiple kinase signals to control DNA replication initiation and fork progression. *Proceedings of the National Academy of Sciences*, *111*, E1899–E1908.

Sheu, Y.-J., & Stillman, B. (2006). Cdc7-Dbf4 phosphorylates MCM proteins via a docking site-mediated mechanism to promote S phase progression. *Molecular Cell*, *24*, 101–113.

Sheu, Y.-J., & Stillman, B. (2010). The Dbf4-Cdc7 kinase promotes S phase by alleviating an inhibitory activity in Mcm4. *Nature*, *463*, 113–117.

Storici, F., & Resnick, M. A. (2006). The *delitto perfetto* approach to in vivo site-directed mutagenesis and chromosome rearrangements with synthetic oligonucleotides in yeast. *Methods in Enzymology*, *409*, 329–345.

Szybalski, W. (2001). My Road to Øjvind Winge, the Father of Yeast Genetics. *Genetics*, *158*, 1–6.

Tomova, A. A., Kujumdzieva, A. V., & Petrova, V. Y. (2019). Carbon source influences Saccharomyces cerevisiae yeast cell survival strategies: Quiescence or sporulation. *Biotechnology & Biotechnological Equipment*, *33*, 1464–1470.

Varrin, A. E., Prasad, A. A., Scholz, R.-P., Ramer, M. D., & Duncker, B. P. (2005). A mutation in Dbf4 motif M impairs interactions with DNA replication factors and confers increased resistance to genotoxic agents. *Molecular and Cellular Biology*, *25*, 7494–7504.

Wang, Y., Lo, W.-C., & Chou, C.-S. (2017). A modeling study of budding yeast colony formation and its relationship to budding pattern and aging. *PLoS Computational Biology*, *13*, e1005843.

Yamazaki, S., Hayano, M., & Masai, H. (2013). Replication timing regulation of eukaryotic replicons: Rif1 as a global regulator of replication timing. *Trends in Genetics: TIG*, *29*, 449–460.

Yang, C.-C., Suzuki, M., Yamakawa, S., Uno, S., Ishii, A., Yamazaki, S., … Masai, H. (2016). Claspin recruits Cdc7 kinase for initiation of DNA replication in human cells. *Nature Communications*, *7*, 12135.

Yeeles, J. T. P., Janska, A., Early, A., & Diffley, J. F. X. (2017). How the Eukaryotic Replisome Achieves Rapid and Efficient DNA Replication. *Molecular Cell*, *65*, 105–116.

Yoder, T. J., Pearson, C. G., Bloom, K., & Davis, T. N. (2003). The Saccharomyces cerevisiae Spindle Pole Body Is a Dynamic Structure. *Molecular Biology of the Cell*, *14*, 3494–3505.

Yuan, Z., Georgescu, R., Bai, L., Zhang, D., Li, H., & O'Donnell, M. E. (2020). DNA unwinding mechanism of a eukaryotic replicative CMG helicase. *Nature Communications*, *11*, 688.

Zegerman, P., & Diffley, J. F. X. (2010). Checkpoint-dependent inhibition of DNA replication initiation by Sld3 and Dbf4 phosphorylation. *Nature*, *467*, 474–478.

Zhao, X., & Rothstein, R. (2002). The Dun1 checkpoint kinase phosphorylates and regulates the ribonucleotide reductase inhibitor Sml1. *Proceedings of the National Academy of Sciences of the United States of America*, *99*, 3746–3751.

Appendix A:

Orc2-Myc ChIP Optimizations at ARS1 and ARS305 Early Origins

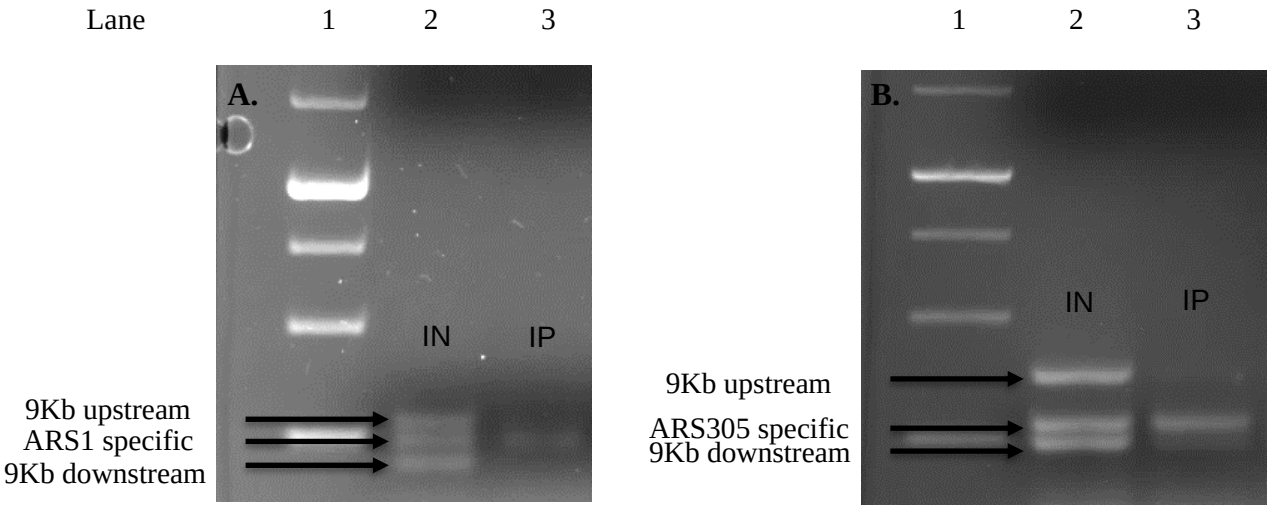

Appendix A Figure 1 Successful Optimization of Asynchronous Orc2-Myc ChIP. Lane 1 of both agarose gels contains a 1kb DNA ladder, containing 13 fragments spanning form 250 – 10,000 base pair sizes. Lane 2 of both agarose gels contains IN samples from Orc2-Myc strain. Lane 3 of both agarose gels contains IP samples from a Orc2-Myc strain. Orc2-Myc was immunoprecipitated by M-280 sheep anti-mouse IgG Dynabeads that were previously incubated with anti-Myc antibodies. Visualization of the 2% agarose gel was completed using a BioRad Chemidoc MP imager. Arrows indicate primer pairs used to amplify each region of interest.

Appendix B

Plasmid Loss Assay Scatter Plot of Standard Score Values

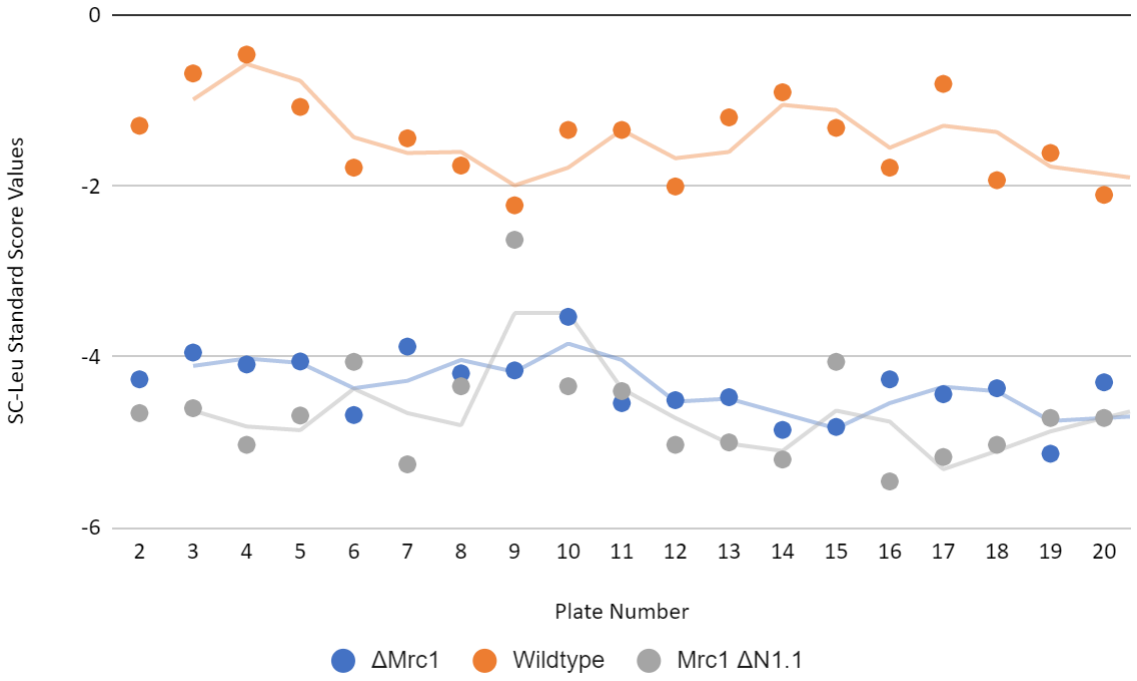

Appendix B Figure 1 Scatter Plot Highlighting the SC-leu Standard Score Values for Various Mrc1 Mutant Strains. Data is based upon two trials of plasmid loss assay. Colony counts for each strain on SC-leu plates was standardized to growth on YPD plates. Trendlines represent a moving average, which shows the average colony counts is similar between Mrc1 ΔN1.1 and ΔMrc1, but vary greatly between Mrc1 ΔN1.1 and the wildtype.